PL-TR-92-2205

ASSESSMENT OF SPACEBORNE LIDAR FOR METEOROLOGICAL ANALYSES

R. G. Isaacs
C. Grassotti
R. N. Hoffman
M. Mickelson
T. Nehrkorn
J.-F. Louis
G. Molnar
B. L. Lindner

Atmospheric and Environmental Research, Inc.
840 Memorial Drive
Cambridge, MA 02139

13 July 1992

Final Report
12 July 1989-12 July 1992

Approved for public release; distribution unlimited

PHILLIPS LABORATORY
Directorate of Geophysics
AIR FORCE MATERIEL COMMAND
HANSCOM AIR FORCE BASE, MA 01731-5000

This technical report has been reviewed and is approved for publication.

MICHAEL K. GRIFFIN
Contract Manager
Satellite Meteorology Branch
Atmospheric Sciences Division

JOSEPH W. SNOW
Chief, Satellite Meteorology Branch
Atmospheric Sciences Division

ROBERT A. McCLATCHEY
Director, Atmospheric Sciences Division

This document has been reviewed by the ESD Public Affairs Office (PA) and is releasable to the National Technical Information Service (NTIS).

Qualified requestors may obtain additional copies from the Defense Technical Information Center. All others should apply to the National Technical Information Service.

If your address has changed, or if you wish to be removed from the mailing list, or if the addressee is no longer employed by your organization, please notify PL/IMA, Hanscom AFB, MA 01731. This will assist us in maintaining a current mailing list.

Do not return copies of this report unless contractual obligations or notices on a specific document requires that it be returned.

REPORT DOCUMENTATION PAGE

Form Approved
OMB No 0704-0188

1. AGENCY USE ONLY (Leave blank)	2. REPORT DATE	3. REPORT TYPE AND DATES COVERED
	13 July 1992	Final (12 July 1989-12 July 1992)

4. TITLE AND SUBTITLE
Assessment of Spaceborne Lidar for Meteorological Analyses

5. FUNDING NUMBERS
PE 35160F
PR 6770 TA 17 WU AR
Contract F19628-89-c-0137

6. AUTHOR(S)
R.G. Isaacs, M. Mickelson, G. Molnar, C. Grassotti*, T. Nehrkorn, B. L. Lindner, R.N. Hoffman, J-F. Louis

7. PERFORMING ORGANIZATION NAME(S) AND ADDRESS(ES)
Atmospheric and Environmental Research, Inc.
840 Memorial Drive
Cambridge, MA 02139

8. PERFORMING ORGANIZATION REPORT NUMBER

9. SPONSORING/MONITORING AGENCY NAME(S) AND ADDRESS(ES)
Phillips Laboratory
Hanscom AFB, MA 01731-5000

Contract Manager: Michael Griffin/GPAS

10. SPONSORING/MONITORING AGENCY REPORT NUMBER
PL-TR-92-2205

11. SUPPLEMENTARY NOTES
* Now at Atmospheric Environment Service, Dorval, Canada

12a. DISTRIBUTION/AVAILABILITY STATEMENT
Approved for public release; distribution unlimited

12b. DISTRIBUTION CODE

13. ABSTRACT *(Maximum 200 words)*

This report summarizes results of a basic research program to investigate and develop advanced techniques for obtaining and applying meteorological parameters from spaceborne lidars. The focus of this program was to identify potentially inexpensive lidar sensor concepts which provide maximum paybacks in improvements to numerical weather prediction (NWP) model performance.

As the result of a trade-off of potential lidar systems for measuring meteorological parameters such as temperature, moisture, and winds, it was determined that maximum payback for NWP could be achieved by improving the accuracy and coverage of wind observations. Since they will be available from a polar orbiter, coverage will be increased, especially for extratropical areas. The lidar will produce winds wherever there is a cloud and will likely provide boundary layer winds from maritime aerosol backscatter. The assessment of the impact of candidate satellite lidar observation concepts on numerical weather analysis and prediction models was performed through a series of observing system simulation experiments (OSSEs).

In addition to NWP model impacts, the fusion of potential lidar sensor system data with that from the current Defense Meteorological Satellite Program (DMSP) suite of passive sensors was considered. Special emphasis was placed on investigating active/ passive data fusion approaches for improving the retrieval of atmospheric temperature and moisture profiles and the analysis of clouds (i.e. nephanalysis) in support of tactical and strategic operations.

14. SUBJECT TERMS
Lidar, Winds, Temperature Profiles, OSSEs, DMSP, Clouds, Retrievals

15. NUMBER OF PAGES
54

16. PRICE CODE

17. SECURITY CLASSIFICATION OF REPORT	18. SECURITY CLASSIFICATION OF THIS PAGE	19. SECURITY CLASSIFICATION OF ABSTRACT	20. LIMITATION OF ABSTRACT
Unclassified	Unclassified	Unclassified	SAR

TABLE OF CONTENTS

LIST OF FIGURES

LIST OF FIGURES (Continued)

LIST OF TABLES

1. INTRODUCTION

This final report summarizes the overall results of a basic research program supported by the Phillips Laboratory, Geophysics Directorate, Satellite Meteorology Branch and conducted by Atmospheric and Environmental Research, Inc. to investigate and develop advanced techniques for obtaining and applying meteorological parameters from spaceborne lidars. The focus of this program was to identify potentially inexpensive lidar sensor concepts which provide maximum paybacks in improvements to numerical weather prediction (NWP) model performance. The assessment of the impact of candidate satellite lidar observation concepts on numerical weather analysis and prediction models was performed through a series of observing system simulation experiments (OSSEs).

As the result of a trade-off of potential lidar systems for measuring meteorological parameters such as temperature, moisture, and winds, it was determined that maximum payback for NWP could be achieved by improving the accuracy and coverage of wind observations. To achieve this goal, two radically different instrument concepts were identified: (a) a combined stereo imager and cloud top lidar based on stereoscopic principles, and (b) a low power Doppler lidar. The stereo lidar will essentially provide super accurate height assignments of CDWs (since image correlation techniques will also be used). Since they will be available from a polar orbiter, coverage will be increased, especially for extratropical areas. The Doppler lidar will produce winds wherever there is a cloud and will likely provide boundary layer winds from maritime aerosol backscatter. Both instrument concepts provide similar atmospheric wind measurement capabilities.

In addition to NWP model impacts, the fusion of potential lidar sensor system data with that from the current Defense Meteorological Satellite Program (DMSP) suite of passive sensors was considered. Special emphasis was placed on investigating active/ passive data fusion approaches for improving the retrieval of atmospheric temperature and moisture profiles and the analysis of clouds (i.e. nephanalysis) in support of tactical and strategic operations.

This report is divided into six sections. The background section (Section 2) provides a brief overview of the history of lidar simulation experiments to date and discusses a possible alternate measurement scenario for improving NWP via a "scaled down" lidar system. Section 3 provides a brief description of possible lidar sensors for meteorological applications and provides a top down, trade off of candidate lidar observing

systems based on a subjective evaluation of projected NWP impact and cost. Section 4 discusses the lidar "scaled down" lidar OSSE and its results. Section 5 treats fusion of lidar data with that from existing passive sensors for two different applications: (a) temperature retrieval, and (b) detection and analysis of thin cirrus cloud. Conclusions are presented in Section 6.

2. BACKGROUND

Since the advent of meteorological satellites a quarter of a century ago, our space-based perspective of the earth's atmosphere-ocean system has been acquired almost exclusively employing passive imagers and sounders. From the earliest single channel cloud imagers to contemporary multispectral scanners and sounders, passive sensor systems have undergone continuous evolution with each succeeding generation of instrument resulting in higher spectral resolution, narrower fields-of-view, and improved detector sensitivity. These advances have been manifested in more accurate and spatially resolved measurements of desired meteorological fields such as those of cloud, temperature, moisture and winds. To date, passive systems have been the key components of the deployed meteorological sensor complement of the Defense Meteorological Satellite Program (DMSP). While affording certain advantages characteristic of a mature technology regarding weight, power, reliability, and cost, passive sensors are not without their inherent instrumental deficiencies. Among these are intrinsic physical limitations on attainable accuracy and vertical resolution and the inability to provide operationally useful measurements of some desired observables.

In order to effectively fulfill its global mission, the Department of Defense (DoD) has established specific observational requirements for the acquisition of high quality geophysical and meteorological data. Among the stated specifications for each desired parameter are coverage area, horizontal and vertical resolutions, mapping accuracy, and the range, accuracy, and precision of the measurement. Temporal specifications include the data refresh period or frequency and the measurement's timeliness. While extant satellite-borne passive sensors partially satisfy some of these needs, remaining gaps in operational observational capabilities make it prudent to consider alternative remote sensing technologies. Active remote sensor systems known as lidars have the potential to bridge some of these gaps, particularly those due to the inability to measure a given parameter using passive means or deficiencies in accuracy and resolution. Thus, the development of space

qualified laser-based sensor systems for actively probing the atmosphere promises to significantly enhance the state-of-the-art of satellite remote sensing.

Numerical weather prediction (NWP) technology and practice have also evolved significantly since their operational beginnings in the 1950s and 1960s. Inferences of atmospheric temperature and moisture, clouds, precipitation, winds, and surface properties are currently made from a variety of passive visible, infrared, and microwave satellite sensors. For global NWP it is primarily the retrieved temperature profile and wind data which are used. The usefulness of other geophysical parameters for NWP is not well established and is largely untested, although a great many retrieval methods have been proposed or developed for a variety of potentially interesting parameters. Moisture variables - that is, specific humidity, clouds and precipitation - are retrievable and are potentially very useful, but are not easily assimilated by current methods. It is theoretically possible to retrieve specific humidity profiles by using methods analogous to those used to retrieve temperatures. However, results to date with available sensors have not been wholly satisfactory. A variety of other meteorological parameters which may be used for NWP are retrievable. These include winds at the surface from microwave sensors and cloud drift winds aloft, as well as other surface properties, such as soil moisture, albedo, snow cover, temperature, and fluxes. Positive impact of current satellite observing systems on global NWP has been demonstrated, especially in the southern hemisphere where conventional data sources are limited. Increasing the accuracy and vertical resolution of the sensors and improving the retrieval and assimilation systems should lead to better forecasts. We believe, nevertheless, that only a small part of the potential usefulness of satellite remote sensing for global NWP has been realized and that lidar sensor systems may play a significant role in this evolution. For example, previous OSSEs with the GL GDAS (Hoffman et al., 1990) using a DWL system which returns complete wind profiles (WINDSAT) have shown significant positive impact upon analyses and forecasts of both height and wind relative to control experiments. Other investigators using different assimilation systems have also found WINDSAT data useful to varying degrees (Arnold et al., 1985; Atlas et al., 1985; Dey and Morone, 1985).

Currently, NASA is in the process of defining the instrument and platform characteristics of the Laser Atmospheric Wind Sounder (LAWS) as part of the Earth Observing System (EOS) initiative. As presently defined (Curran, 1989) the LAWS instrument would be a relatively high power active DWL sensor (10 J pulse) operating at 9 μm, potentially capable of returning complete profiles of horizontal wind from the top of

the troposphere to cloud top with a vertical resolution of approximately 1 km and a horizontal resolution of 100 km. Anticipated accuracies for horizontal vector winds are on the order of 1-5 ms^{-1} rms (Baker, 1992).

However, there are legitimate concerns regarding the weight and power requirements of an instrument such as LAWS. Secondly, the ability of the instrument to obtain complete vertical profiles of wind through the troposphere is critically dependent upon the presence of sufficient backscattering aerosol. Data from the Global Backscatter Experiment (GLOBE) should help resolve this, but the answer is far from certain Menzies and Tratt, 1991; Spinhirne et al., 1991). Finally, the size, weight and power of the instrument are all directly proportional to its ultimate development cost. In this regard, the recent restructuring of the EOS program has placed the LAWS instrument in the category of instruments for which funding has not yet been identified (*Earth Observer, 4*, 1, p. 5)

The approach adopted for this study is to assess the NWP utility of a downscaled (i.e. lower power and weight) DWL instrument which addresses these concerns (note that the primary LAWS objective is global change monitoring). The scaled back instrument could potentially be smaller, operate at lower power levels (1 J pulse), and work at a near-infrared wavelength (see Table 1). These characteristics would lower the cost, decrease demands upon the host platform, and, relative to a comparable infrared lidar, increase the backscatter signal. Since the instrument is operating at lower power, we have assumed that visible returns will only occur at or near "hard" targets where backscattered signal is sufficient. These targets are cirrus cloud, the tops of other clouds and marine boundary layer aerosol.

Table 1. Lidar System Parameters

Parameter	Value
Wavelength	2.1 μm
Sensor altitude	824 km
Scan angle	45 degrees
Scan period	5 s
Pulse energy	1J
Pulse duration	.7 μs
Noise bandwidth	2.2 MHz
Pulse rate	10 Hz
Optics diameter	.5 m
Total efficiency	0.75

Finally, we note that range gating of the laser pulse itself can allow fairly accurate estimation of the target height. Although not utilized in the experiments conducted here this could be used to infer cloud top height which might also be incorporated into a data assimilation system.

3. TRADE-OFF OF POTENTIAL LIDAR OBSERVING SYSTEMS

3.1 Lidar Measurement Techniques

Several of the geophysical parameter requirements alluded in Section 2 can only be met by using active spaceborne lidar sensors. Ultimately, lidars should be able to satisfy many of the operational goals (accuracy, resolution, etc.) defined for these parameters. No single lidar sensor, however, can satisfy all of the observational requirements including temperature and moisture profiles, winds, cloud tops, etc. Instead, several diverse lidar measurement techniques and algorithms must be utilized. In order of increasing instrument complexity, these techniques include:

- Backscatter lidar
- Differential absorption lidar (DIAL)
- Doppler wind sensors

3.1.1 Backscatter lidar

Backscatter lidar is loosely defined here as a variety of measurement methods which utilize the signal backscattered by "hard" targets or atmospheric constituents without regard to the precise spectral characteristics of the transmitted or returned signal. Changes in frequency between the transmitted and returned signal are ignored. This category comprises the following techniques:

- Cloud height ranging and phase discrimination
- Atmospheric transmittance or extinction measurements
- Aerosol measurement
- Sea state
- Density measurements from which temperature profiles can be derived

These methods are listed roughly in order of increasing complexity and decreasing precision for a given system parameter. Clearly, measurement of cloud top heights are relatively simple, requiring only the measurement of the time delay between pulse transmission and return from the cloud top, which acts as a hard target for optically thick clouds. Cloud phase discrimination requires additional optical components to separate the polarization components of the backscattered signal. Aerosol measurements require that assumptions be made to separate the aerosol and molecular components of the returned signal. Other assumptions are necessary to estimate transmittance over the ocean. Still more assumptions are required to estimate atmospheric density and temperature profiles.

Detecting the presence of clouds and ranging of cloud top altitudes can be readily carried out with high accuracy by a relatively low power orbiting lidar. Measurements of lidar-derived cloud top heights together with passive cloud top temperature measurements can determine precisely one point in a temperature profile. Consequently, these measurements could enhance passive radiometric measurements of temperature profiles. Lidar derived cloud heights could also be used to assign altitudes to wind velocity vectors determined by passive cloud tracking. Cloud detection is a relatively simple task as there exists an extremely large gradient in both backscatter and transmission at the cloud - clear air boundary.

3.1.2 Differential absorption lidar

In the presence of molecular absorption lines, the transmittance term in the lidar equation can vary appreciably over very small changes in frequency. This strong frequency dependence of the molecular absorption coefficient can be exploited to yield information on absorber concentration and atmospheric temperature. The basic principal of the DIAL technique is as follows. A tunable laser is used to emit nearly simultaneous pulses over an identical path at two different frequencies; one centered on an absorption line, the other off-line but close enough in frequency such that the effect of other attenuation mechanisms and aerosol backscatter are approximately equal for both frequencies. The ratio of the received signals yields the line absorption coefficient K:

$$K(R) = \frac{1}{2\Delta R} \ln \frac{P_r(\upsilon_\ell, R - \Delta R/2) \cdot P_r(\upsilon_o, R + \Delta R/2)}{P_r(\upsilon_o, R - \Delta R/2) \cdot P_r(\upsilon_\ell, R + \Delta R/2)} \qquad (2)$$

where υ_ℓ and υ_o signify the on-line and off-line frequencies respectively (see Hogan et al., 1983). For the case of collision broadened absorption lines at line center, the amount of absorption is a function only of temperature and absorber concentration. Some absorption lines are very sensitive to temperature while others are only weakly dependent on temperature. Immediately two strategies are apparent: (a) selecting spectral lines with a small temperature dependence, the concentration of the absorbing gas can be determined, and (b) selecting an absorbing gas with a uniform concentration and an absorption line with a high temperature sensitivity, measurements of temperature can be made. For the case of absorption lines which are dominated by Doppler broadening, only the first approach is feasible - solving for number density of the absorbing gas. For all of the approaches, pressure estimates are necessary although the pressure dependence of the linewidth is a weak one for most purposes. If two lines, one with a weak temperature dependence, the other highly sensitive to temperature, can be found close enough in frequency, a three frequency technique may be employed to give simultaneous temperature and concentration measurements. This technique compares two on-line pulses with a single off-line pulse to extract the two quantities simultaneously.

3.1.3 Doppler wind lidar (DWL) sensors

Aerosols suspended in the atmosphere can serve as wind tracers for lidar measurements. A photon backscattered by an aerosol particle moving at a wind velocity (v) in the line-of-sight will experience a Doppler shift in frequency of magnitude $(Dn/n) = (2v/c)$, where c is the speed of light. Photons scattered by particles moving toward the observer in the line-of-sight will experience an increase in frequency, while those scattered by particles receding from the observer will display a decrease in frequency. The Doppler shift caused by aerosol backscattered of a highly stable quasi-monochromatic laser beam could be spectrally analyzed to yield the line-of-sight component of wind velocity. In practice, measuring winds by this method is very difficult because of several facts:

- The doppler shift is extremely small - a 1 ms^{-1} wind (line-of-sight) results in ~$3x10^{-1}$nm shift at 0.5 μm, or ~$6x10^{-5}$nm at 10 μm.

- The spacecraft velocity, which is about 8 km/sec, also contributes to the Doppler shift. The contribution of this velocity along the line-of-sight of the measurement must be determined to a high accuracy. This places stringent requirements on instrument pointing knowledge and spacecraft attitude.

- The aerosol backscattered signal is often quite small (particularly in the altitude range of 5-12 km where winds are very important) and at some frequencies is dwarfed by the much stronger molecular backscattered signal.

There are two major techniques using coherent and incoherent detection to determine wind velocity in this way. The coherent method uses heterodyne detection; mixing the backscattered signal with a local oscillator to yield a beat frequency proportional to the Doppler shift. The incoherent technique measures spectral shifts using a Fabry-Perot interferometer with an array-type detector. The relative advantages and disadvantages of the two systems are discussed by Salvetti (1987) and Baker and Curran (1988). These three works also summarize potential implementations of DWLs.

It is now considered technically feasible to measure wind profiles from space by measuring the Doppler shift of a transmitted laser pulse (Salvetti, 1987; Curran et al., 1988). With a strong enough signal the reflected pulse may be range gated to yield vertical resolution of 1 km or better. The strength of the reflected signal depends principally on the energy transmitted and the reflectivity of the atmospheric volume being sampled. Since the laser may be focused to a very fine solid angle, horizontal resolution as fine as desired (down to scales of meters) may be obtained. Further, the lidar measurements are a direct measure of the line of sight (or radial) velocity. Thus, if the reflected signal strengths are sufficient any reasonable desired accuracy might be obtained by this technique.

Two measurements of the same atmospheric volume from different viewing angles, along with the assumption that vertical velocities are negligible, are required to infer the (u, v) wind components. The simplest method of accomplishing this is to use a conical scan pattern (cf. Fig. 19 of Curran et al., 1988).

The global distribution of aerosol is not well known. Since the aerosol concentration directly effects the atmospheric reflectivity to the lidar signal, the relationship of the DWL errors to the transmitted energy cannot be reliably predicted. However, in the experiments proposed here, we need only assume a given error level. The equivalent transmitted energy might be calculated by assuming some aerosol distribution.

3.2 Candidate Lidar Observing Systems

We developed and analyzed a list of potential lidar observing systems with the goal of investigating low cost alternatives to the full scale Windsat concept described above. Table 2 summarizes these lidar observing systems concepts. The table has been annotated to identify advantages and disadvantages from the NWP modeling perspective and to provide a rough order of magnitude (ROM) cost estimate. Cost estimates are based on those developed by AER and RCA AstroSpace Division (now GE).

The measurement techniques have been divided into three categories which roughly correlate with cost and approach: (a) elastic backscatter, (b) differential absorption lidar (DIAL), and (c) WINDSAT. A number of alternative measurement scenarios are presented within each category. Elastic backscatter instruments are quite feasible with current technology. DIAL will be very expensive while WINDSAT type lidars will be more expensive still. However, with regard to the WINDSAT type instrument our previous OSSE has indicated that potential impact will be large.

The elastic backscatter category provides height resolution of cloud targets. For example, a cloud height and an imager equivalent black body brightness temperature (EBBT) provides a temperature height observation (Table 2, type A.1). Such single layer temperature data, by itself, however, will not have a large impact. Alternatively, this single level data could be used in a data fusion approach to constrain the retrieval of temperature from a passive sounder in the manner suggested by Weinman (1985) (Table 2, type A.2). This would increase the accuracy of the retrieved profile. Pressure assignment error would be a problem of this approach (see Section 2.3). Conceptually, this experiment would be analogous to redoing our previous SSMSAT experiment (Hoffman et al., 1990), however, with smaller random errors in the temperature profile retrievals. Cloud top height information could also be used to more accurately assign the heights of cloud drift winds (CDW) (Table 2, type A.3). Again, single level data will have a smaller impact than a full profile. The last elastic backscatter concept combines data from a stereoscopic imager and a backscatter lidar to provide cloud top topography and cloud drift winds (Table 2, type A.4). However, since all cloud tops would be sampled, there will potentially be more of this data coverage than that available from conventional CDW.

Table 2. Candidate Lidar Observing Scenarios

	Technique	Advantages	Disadvantages	Cost
A	Elastic Backscatter			
A.1	Cloud Height + Imager EBBT	Yields temperature height pair.	Single level data pressure assignment	$
A.2	Passive Temp. Profile + A.1	Refine temperature profile.	Pressure assignment	$
A.3	Cloud Height + CDW	Improve CDW height assignment.	Single level data	$
A.4	Cloud Height + Stereo Imager	Cloud topography and cloud winds.	Single level data	$
B	DIAL			
B.1	Water Vapor	High accuracy/vertical resol. moisture through troposphere.	Pressure assignment RH problem	$$
B.2	Temperature	High accuracy/vertical resol. temperature through troposphere.	Pressure assignment	$$
B.3	Passive Sounder + B.1/B.2	Complementary vertical resolution; passive more accurate above lower troposphere.	Pressure assignment	$$
C	WINDSAT			
C.1	Nominal WINDSAT	Done already.	Done already	$$$
C.2	Two Satellites	Double coverage.	System cost	$$$$
C.3	Tropical Only (Dey et al.)	Energy saving. Complements extratropical passive sounding data.	-	$$$
C.4	Ocean Only	Energy saving. Complements RAOB network.	-	$$$
C.5	Vertical/Horizontal Resolution Trade	Energy saving. Adjustment theory: external mode for wind data most useful.	-	$$$
C.6	Denied Data	Satellite only by region for contingency planning.	-	$$$
C.7	Single Layer Cloud Top WINDSAT	Energy saving.	Single level data	$$

DIAL sensors will provide highly accurate, vertically resolved temperature and moisture profiles (Table 2, type B.1,2). For use in NWP there will be a significant problem with pressure assignment, but they will certainly complement the low vertical resolution capabilities of passive sounders and could be combined with these data to extend the horizontal coverage of the DIAL sensor (Table 2, type B.3).

All of the WINDSAT experiments except for the nominal experiment already conducted (Table 2, type C.1) are based on energy conservation or data coverage change scenarios. The second (expensive) candidate is the use of two sensors (Table 2, type C.2) which should yield a large positive NWP impact. Experiments C.3,4,6 explore the trade-off between real coverage and available power. For these experiments we expect little degradation of our nominal WINDSAT results. Experiment C.5 is a test of adjustment theory which trades off vertical and horizontal resolution. According to Daley (1980) optimal initial state specification theory, winds are most important for the small horizontal scales and largest vertical scales and conversely for temperature. This suggests high vertical resolution is wasted in a wind observing system. However in a multivariate analysis system winds affect the temperature initial state and vice versa so that relevance of adjustment theory for practical NWP in the extratropics is not so clear cut. This experiment would test this hypothesis.

From this list of candidate lidar observing scenarios we chose to perform an OSSE based on a scenario much analogous to something like A.4 or C.7 (Table 2). This would provide presumably high quality winds and accurate height assignment, but only at cloud top for water clouds, through cirrus layers, and in the boundary layer where it is assumed that aerosol backscatter is sufficient. One of the main advantages of this observational philosophy is that the potential global coverage of high quality winds is enhanced over that obtainable from CDWs.

4. Simulation of Simple Lidar Impacts on NWP

4.1 Background

Observing systems simulation experiments (OSSEs) provide a powerful tool to assess the impact of proposed satellite borne observing systems on meteorological applications models (Arnold and Dey, 1986). Here we provide a brief summary of the results of an OSSE conducted to assess the impact of data from a low power lidar wind

sensor on the forecast accuracy of a global spectral numerical weather prediction (NWP) model, the Air Force Geophysics Laboratory Global Data Assimilation System. An extensive report on these results has been published as Scientific Report No. 1 of this contract (Grassotti et al., 1991).

The proposed lidar instrument would be operating at near-infrared wavelengths thereby increasing the backscatter signal relative to a comparable infrared lidar. Since it would also operate at lower energy, its resolving power is not expected to be as great and retrieved wind profiles are not likely to be as complete, with measurements primarily at or near cloud tops, from cirrus return, and in the marine boundary layer. This instrument may be seen as a potentially lower cost alternative to some of the other lidar instruments which are currently planned such as the Laser Atmospheric Wind Sounder (LAWS) (see Huffaker et al., 1984). The trade-off is that between system complexity and potential payback measured in terms of positive impact on numerical weather prediction (NWP) forecast accuracy. For the more complex lidar wind sounder, impacts can be ascertained from our previous experiment based on the WINDSAT concept (Hoffman et al., 1990).

4.2 Approach

An extended 20 day forecast of the ECMWF grid point model (nature run) serves as ground truth for cloud diagnosis and for verification. The simple lidar wind sounding instrument has been assumed to be aboard the DMSP polar orbiting platform with observational coverage similar to the SSM/T sounder. Three types of returns are treated: (1) cirrus cloud, (2) liquid water cloud, and (3) marine boundary layer aerosol. Two line of sight velocity measurements, with their own intrinsic errors are required to uniquely determine the two-dimensional horizontal wind vector. Errors of the u and v components are treated as a function of both distance to the satellite subtrack as well as the orientation of the satellite track with respect to lines of latitude and longitude. This results in measured wind profiles which contain observations at one or several levels, but never complete profiles, and which reflect the local geophysical conditions (i.e. cloudiness). The errors associated with each observation are a function of the viewing geometry and the actual source of the lidar backscatter: cirrus, water cloud, or marine boundary layer aerosol. Using the Geophysics Laboratory (GL) Global Data Assimilation System, we insert the simulated wind data at 6 hour intervals into the assimilation system for a period of 7 days. Forecasts of 4 days in length are run using the GL Global Spectral Model (Brenner et al.,

1982, 1984) with initial conditions provided by analyses valid at various points during the assimilation run.

4.3 OSSE Procedure

The procedure is summarized in Fig. 1, which shows the control simulation, the lidar simulation and respective forecasts with the nature run or truth initial state.

4.4 Data Simulation

There are essentially two steps in the process: (a) identifying where lidar data is available and extracting it from the nature run (perfect lidar data) and (b) assigning appropriate measurement error or noise to the lidar data to accomplish a realistic simulation.

4.4.1 Perfect lidar data

As a preliminary to accomplishing step (a), fields of temperature, relative humidity, height, and u and v wind components have been extracted from the OSSE nature run for each 6 hour time period of the assimilation cycle. This grid uses the orbital geometry of the DMSP and is consistent with a 45 degree scan given a 1700 km swath width. Cirrus clouds are diagnosed from both the relative humidity and temperature profile at the observing location. Liou et al. (1990) have proposed a simple criterion for the presence of cirrus cloud. Ice clouds are present if both the relative humidity and temperature fall above and below their critical values, respectively. A threshold relative humidity is calculated as a function of ambient temperature. We have modified the criterion to reproduce the fall time period zonal climatology of the SAGE data results of Woodbury and McCormick (1986). We have also assumed that cirrus clouds are sufficiently transmissive so that the presence of cirrus does not necessarily preclude returns from lower levels. Liquid water clouds are diagnosed using the Geleyn scheme (Geleyn, 1981) using the same critical relative humidity values as in the nature run. A measurement occurs if the cloud fraction at a particular level as seen from the satellite (assuming random overlap) exceeds a critical value. Finally, a measurement in the marine boundary layer results if, again, the fraction of the lowest layer seen from above exceeds a critical value. This measurement is considered to be an average of the wind at the lowest two mandatory pressure levels (1000 and 850 mb).

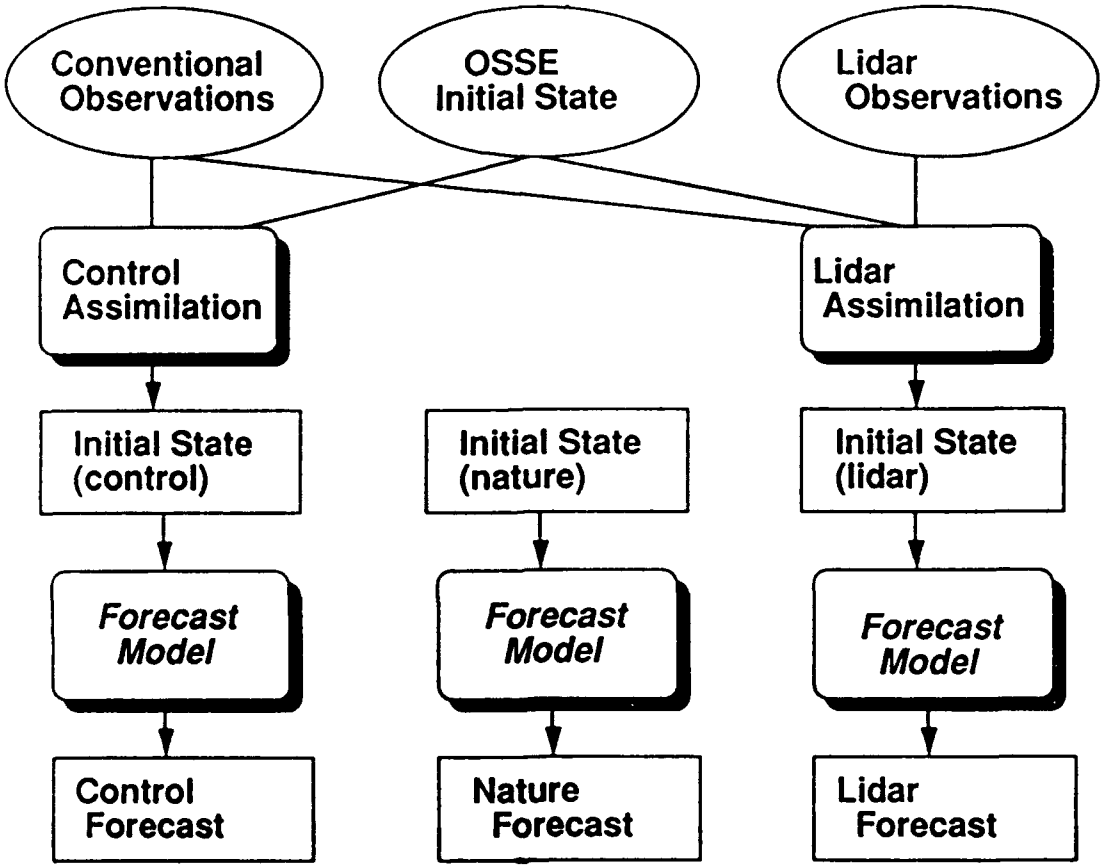

Figure 1: Lidar OSSE Procedure

4.4.2 Lidar data errors

Lidar wind data errors will depend on the sensor characteristics as well as orbital data. To provide an estimate of wind vector errors for a simple lidar, an instrument simulation model has been applied. Optical properties of the clouds are required to ultimately assign a wind retrieval error. Properties of liquid water clouds assume a simple stratus or stratocumulus drop size distribution. The boundary layer aerosol model is a marine boundary layer model. We have not considered the relative humidity dependence of the aerosol size distribution. The estimation of cirrus optical properties including extinction and the desired lidar backscatter cross sections were based on the parameterization of the cirrus particle size spectrum by Heymsfield and Platt (1984). This results in one class of size distribution corresponding to "warm" and "cold" cirrus, respectively. This is consistent with a change in lidar extinction to backscatter ratio noted by Platt and Dilley (1981). We exploit this dependence to simplify our treatment of the temperature dependence of the cirrus backscatter and assignment of simulated wind errors. To calculate backscatter coefficients we adopt the optical constants for ice from Warren (1984). The backscatter and extinction coefficients corresponding to the temperature dependent size distributions described above are evaluated using the Mie theory algorithm of Shettle (pers. communication). Although the Mie theory is strictly applicable to spherical particles a comparison of asymmetry factors calculated by Takano and Liou (1989) for hexagonal crystals and equivalent ice spheres suggests that, for our purposes, the error is not significant.

4.5 OSSE Results

The specific results of the OSSE are summarized by these specific findings:

Synoptic maps:

- Reduction in analysis and forecast errors of 500 hPa geopotential height in the southern hemisphere by factors of 2-3;
- Most of the data impact on vector wind analysis and forecast in the southern hemisphere with wind vector errors of 20-30 ms^{-1} reduced to 10 ms^{-1};
- Again most impact in the southern hemisphere extratropics with large areas of errors greater than 50% in the CONTROL experiment reduced in the LIDAR analysis. Similar results for humidity forecasts with improved specification of the horizontal motion field leading to a better moisture forecast.

Time evolution of forecast and analysis error:

- Global reduction of the 500 hPa height analysis error by a factor of two (from 25 m to 12 m), most dramatic in the southern hemisphere. A global increase in accuracy for a three day forecast by the equivalent of 12 hours relative to control (36 hours in the southern hemisphere extratropics);
- A thirty percent reduction in the error of the 850 hPa zonal wind component with a forecast predictability improvement in the southern hemisphere of up to 48 hours;
- Consistent positive impact on the analysis of 850 hPa relative humidity in the southern hemisphere with forecast predictability increases of 24 to 72 hours compared to control.

Averaged forecast error:

- Global improvement of the 500 hPa height forecast (compared to CONTROL) by 1 day (2-2.5 days in the southern hemisphere);
- Global zonal wind forecast error improvements of 0.5 and 1 days and at 850 hPa and 200 hPa, respectively (1-1.5 days and 2 days, respectively, in the southern hemisphere);
- Improvements in the 850 hPa humidity forecasts by 1-1.5 days.

We have also performed an OSSE to evaluate the impact of a WINDSAT type instrument (Hoffman et al., 1990). In the examination of southern hemisphere results, a meaningful comparison of WINDSAT and LIDAR impacts can be made. The scaled down LIDAR system reduces 500 hPa geopotential height analysis errors by between 1/2 and 3/4 that of the WINDSAT system. Predictability increases for LIDAR are about one day less than WINDSAT. Zonal wind improvements at 850 hPa from LIDAR are about 1/2 of WINDSAT.

5. ACTIVE PASSIVE DATA FUSION

Data fusion is another possible approach to maximize the utility of lidar energy, in particular some characteristics of lidar systems complement other satellite sensors. In this section we will explore several conceptual ideas for combining information from a variety of sensors with lidar observations. The approaches we will discuss in this section fall into two broad classifications. First there are those systems designed to complement other observing systems. Since the lidar is active, it can probe just those regions most inaccessible to passive sensors. For complementary data, the OI technique is an ideal way

of combining data from different sources. The second broad classification contains those approaches which use lidar's unique capabilities to provide some particular piece of information needed in the retrieval of geophysical parameters from some other system.

While our focus has been the impact of lidar based winds on the analysis and forecasting in the context of NWP, lidar information can also be used to improve the retrieval of other EDRs by exploiting active/passive sensor data fusion approaches. We have explored in some detail approaches to improve the retrieval of two important EDRs which are today obtained using passive data alone. These were: (a) using lidar cloud top height information to supplement a physical retrieval of temperature from SSM/T data; and (b) the use of the lidar to identify the presence of cirrus cloud to enhance the results of passive cloud property retrieval using a state-of-the-art spatial coherence technique. Both of these studies were done as simulations. To summarize the results which we have obtained: both experiments indicated that the lidar data could be used to improve the passive only retrieval.

In the case of the microwave temperature retrieval it was demonstrated that the ability to fix the temperature at cloud top could be used to constrain the physical inversion of temperature from an instrument such as the SSM/T. Operationally, it would be necessary to identify the presence of cloud from a combination of the lidar data and corresponding imagery. The enhancement would only be possible when cloud was present within the field-of-view. While the details need to be worked out. It can be seen that both data sources (i.e. lidar and sounder could be used together).

A problem with current passive cloud analysis approaches is the difficulty in delineating cirrus cloud. Non-unit emissivity cloud is a problem with most approaches. We have illustrated that the availability of lidar data to identify cirrus cloud results in a significant improvement in cloud cover determination for low emissivity cirrus. These results assumed a single cloud layer, however, preliminary results are also provided for a two layered system where one of the layers is a thin cirrus cloud.

5.1 Temperature Profile Retrieval Using Lidar Cloud Top Heights

We examined the degree to which standard physical retrieval techniques would be improved if lidar data were available in addition to the passive sounding data. Lidar provides an accurate temperature retrieval, but only at the altitude of the cloud top.

Nonetheless, this information will improve our retrieval at all altitudes since the weighting function for each channel spans many altitudes, and will therefore be affected by the lidar data.

We simulated the incorporation of lidar data by constraining the retrieval to return the true temperature at the cloud top altitude, and by allowing the retrieval at other altitudes to be impacted by this new information. Specifically, the co-variance matrix is altered so that the temperature of the three layers at cloud top altitude is retrieved independent of the information at other altitudes. Since lidar data is highly accurate, sounding data do not noticeably improve the retrieval at cloud top altitudes. The cross correlations are zeroed for all other layers with the cloud top layers. In addition, the cross correlations for these 3 cloud top layers with themselves are reduced by 10^6 to allow for an exact temperature retrieval at cloud top altitude. The cloud top altitude was allowed to vary to simulate the variety of clouds observed in nature, and to study how this variability affected the retrieval.

Figure 2 compares the errors obtained by the retrieval code when lidar information is ignored to the errors obtained by the retrieval code when lidar information is incorporated. Taking the difference of the errors produced by these two retrieval schemes shows to what degree the original retrieval scheme is improved by using lidar data, which is what we have plotted in Fig. 3. Clearly, the original retrieval scheme is substantially improved at the cloud top altitude (300 mb in this case). The improvement at this altitude is due solely to the addition of lidar data at that altitude, and not to the retrieval technique. However, an overall improvement in the temperature retrieval at other altitudes is also noted, which shows that the overall effectiveness of the retrieval technique is enhanced by the use of lidar data. The retrieval is worse at some levels, but this is due to normal fluctuations present in the atmospheric temperature structure. In other words, the temperature structure in the atmosphere does not follow a smooth lapse rate but has inherent instability and variability on an altitude scale that is too fine for the retrieval to infer (unless more channels are used). But overall, improvement is noted at more altitudes, and with greater importance.

Note that the improvement in the retrieval which results from adding lidar information diminishes with distance from the cloud top. In fact, above 10 mb there is little effect at all. The reason for this is shown schematically in Fig. 4. Those channels which have weighting functions that peak near the cloud top will obviously benefit the most from the addition of the lidar data because the channels obtain a substantial fraction of their

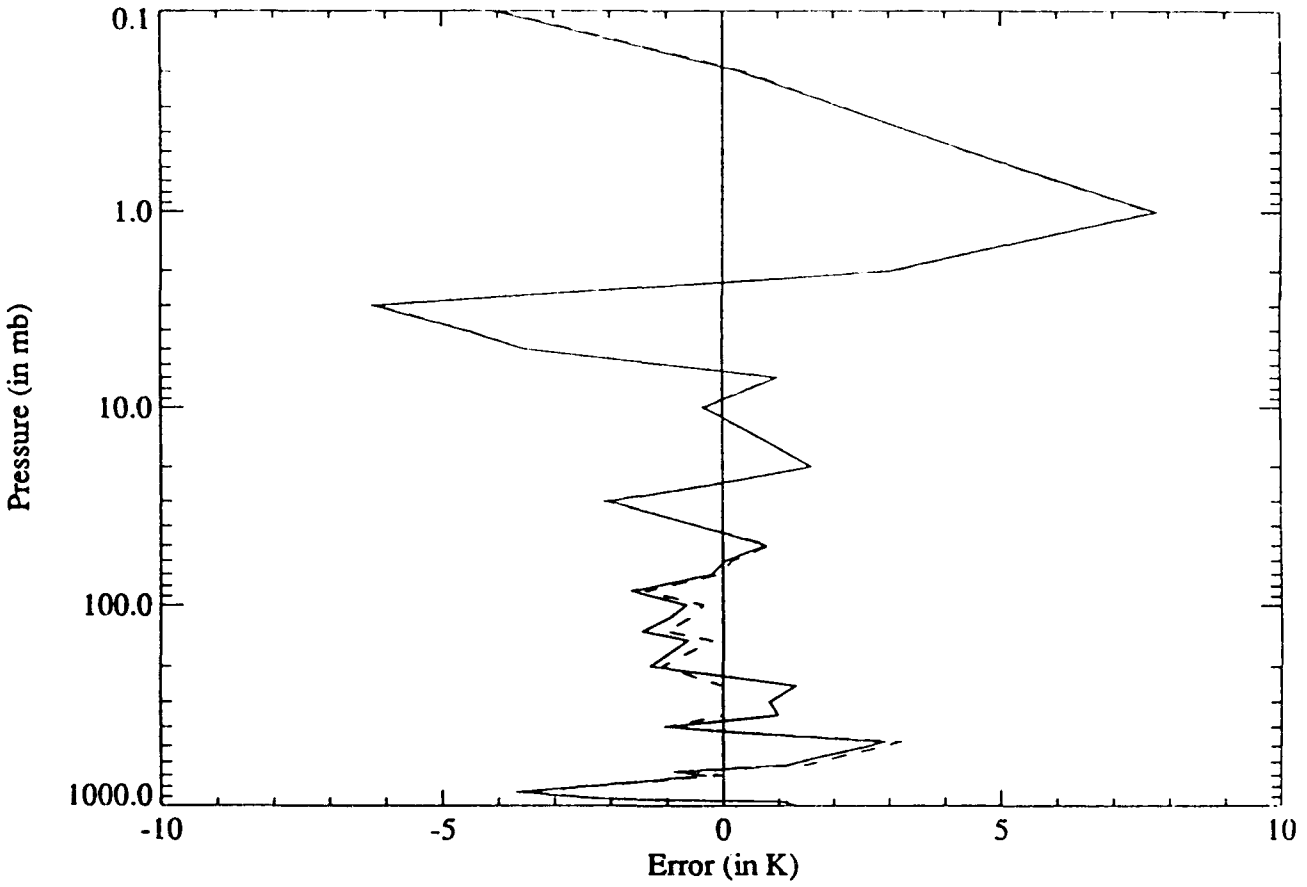

Figure 2: The difference between the retrieved temperature and the true temperature (the error), as a function of pressure. The solid line is for the retrieval scheme ignoring lidar data. The dotted line is for the retrieval scheme including lidar data. The cloud top is at 300 mb.

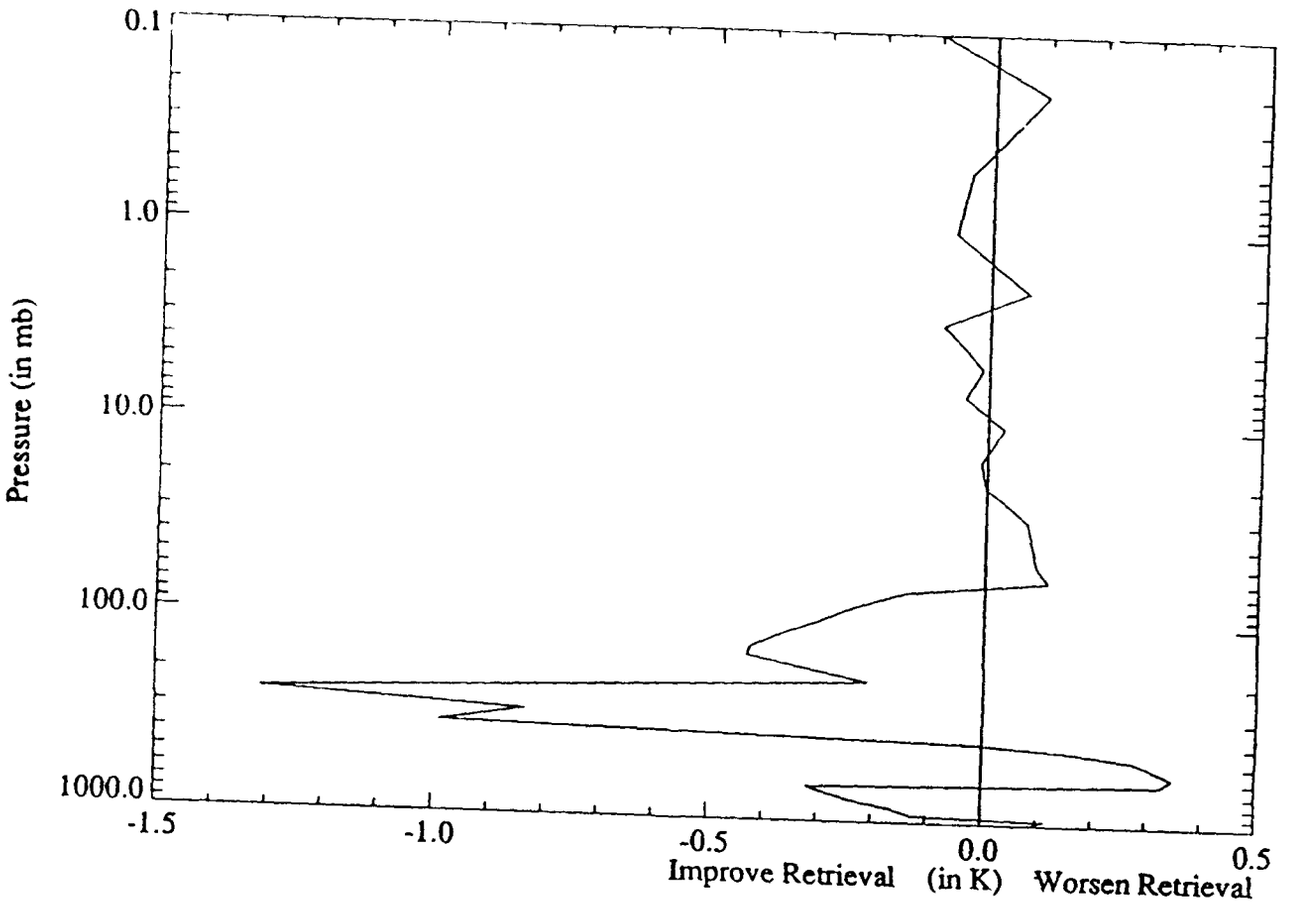

Figure 3: The difference between the error in the retrieval scheme ignoring lidar data and the error in the retrieval scheme including lidar data, as a function of pressure. Inclusion of lidar data improves the retrieval scheme for negative values on the x-axis (i.e. reductions in the error) and worsens the retrieval for positive values. The cloud top is at 300 mb.

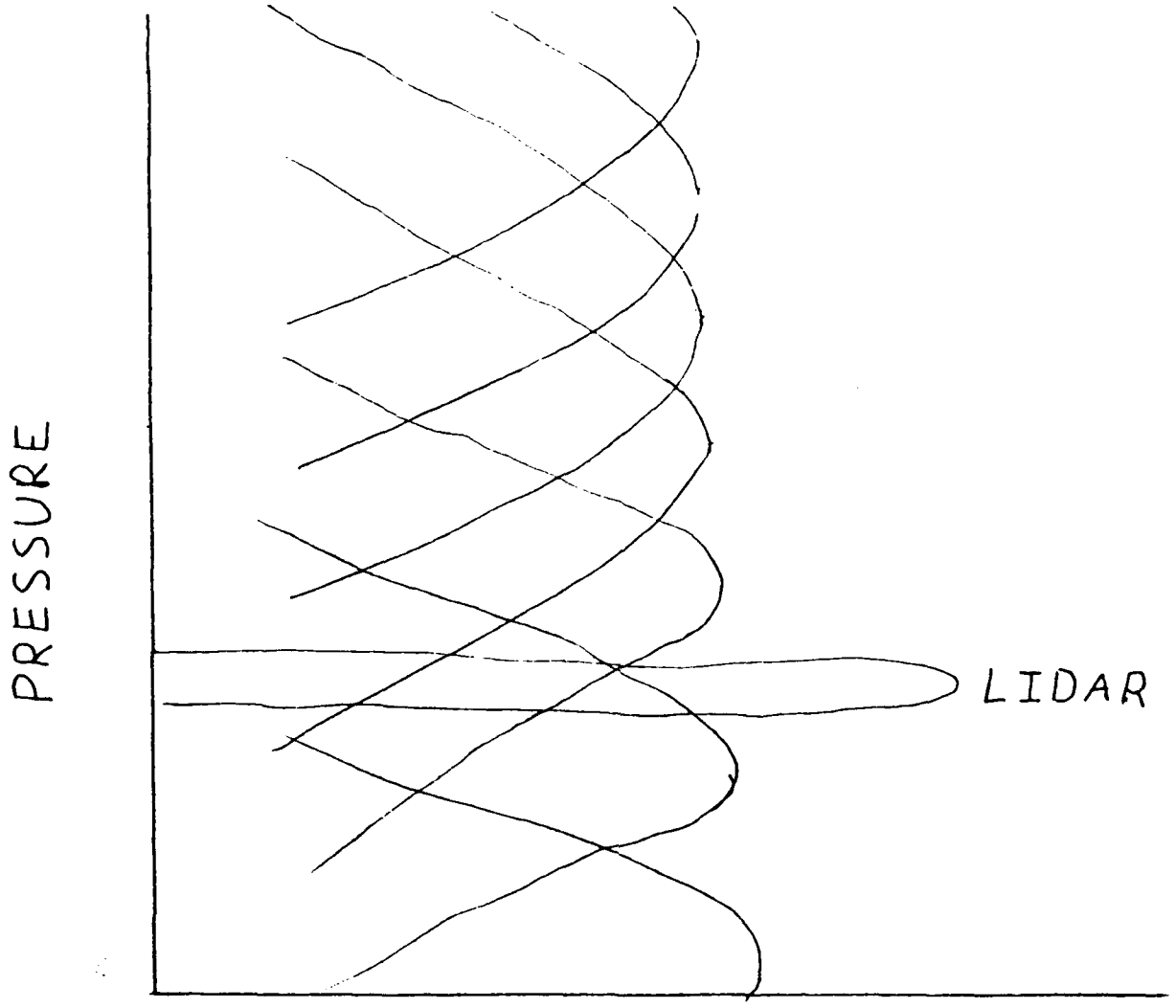

Figure 4: Schematic showing the weighting functions for the seven channels and the weighting function for the lidar data, as a function of pressure. Note that the weighting function for lidar data is narrower in width and stronger at its peak.

weighting function from the cloud top altitude. On the other hand, channels which cover the upper atmosphere, for example, receive only a minor fraction of their weighting function from cloud top altitude (see Fig. 4), which explains why the retrieval of temperature in the upper atmosphere is not noticeably affected by the addition of lidar data.

The degree of the improvement in the retrieval scheme also depends on what cloud top altitude is used. Figures 5 and 6 show the same information as Fig. 3, only with different cloud top altitudes. For all cloud cases we examined, an improvement in the overall retrieval is noted, although the degree of improvement varied. The reason for this variance in improvement is two-fold. One reason has to do with the placement of the cloud top altitude relative to the weighting functions. As shown in Fig. 4, if the lidar information coincides with the peak of a weighting function, then it will be more useful to the retrieval scheme than if the lidar information fell between two weighting functions, where little information is available. In a sense, the addition of lidar data can be thought of as adding another channel, albeit a very accurate channel with a very narrow weighting function. If the lidar "channel" peaks at the same altitude as another channel, then the information is redundant and provides a direct check on the accuracy of the retrieval at that altitude. If the lidar "channel" falls between two weighting functions, then there will be a marked improvement in the retrieval at cloud top altitude, but there will be less of an improvement at other altitudes because the lidar information cannot be as easily assimilated in the weighting functions. This effect can be seen in Fig. 7. The peaks of the weighting functions for 3 channels occur at approximately 100 mb, 300 mb, and 800 mb. As Fig. 7 shows, having lidar information available at those levels results in large improvements in retrieval accuracy, whereas improvements are minimal if the lidar data occurs between the peaks of the weighting functions.

The other reason for the variance in the improvement in the retrieval scheme with the placement of cloud top altitude has to do with whether the lidar information is at an altitude which has "unusual" temperature structure (e.g., a strongly positive lapse rate or a negative lapse rate). Unusual structure such as a small-scale inversion is difficult for a sensor with only 7 channels to resolve, and hence adds to the error at the altitude where this unusual structure occurs. If the lidar information occurs at an altitude where unusual structure occurs, it obviously does a better job of reducing the error.

In summary, we have shown that the addition of lidar data improves our retrieval scheme, even at altitudes other than where the lidar information is taken. The degree of this

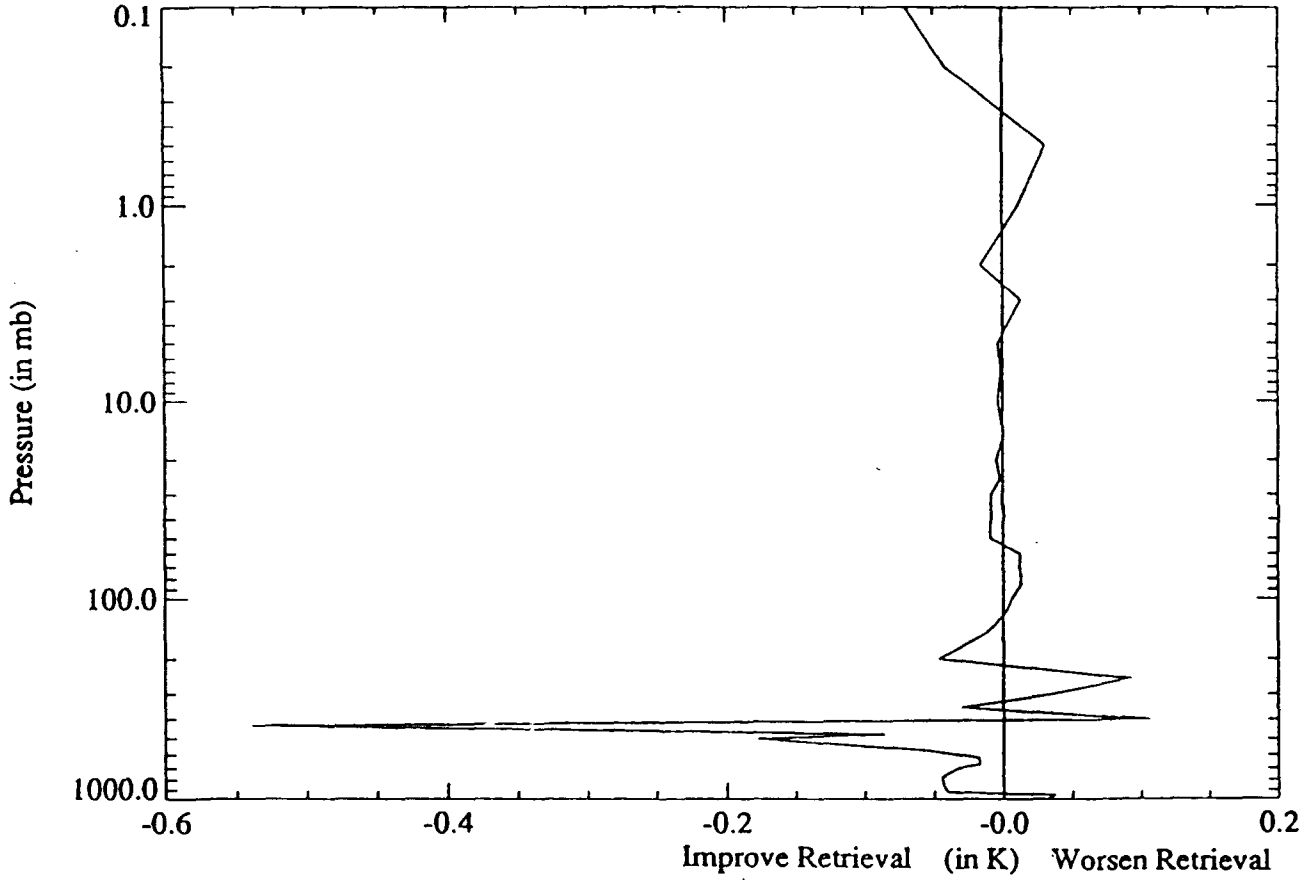

Figure 5: As for Fig. 3 except for a cloud top at 475 mb.

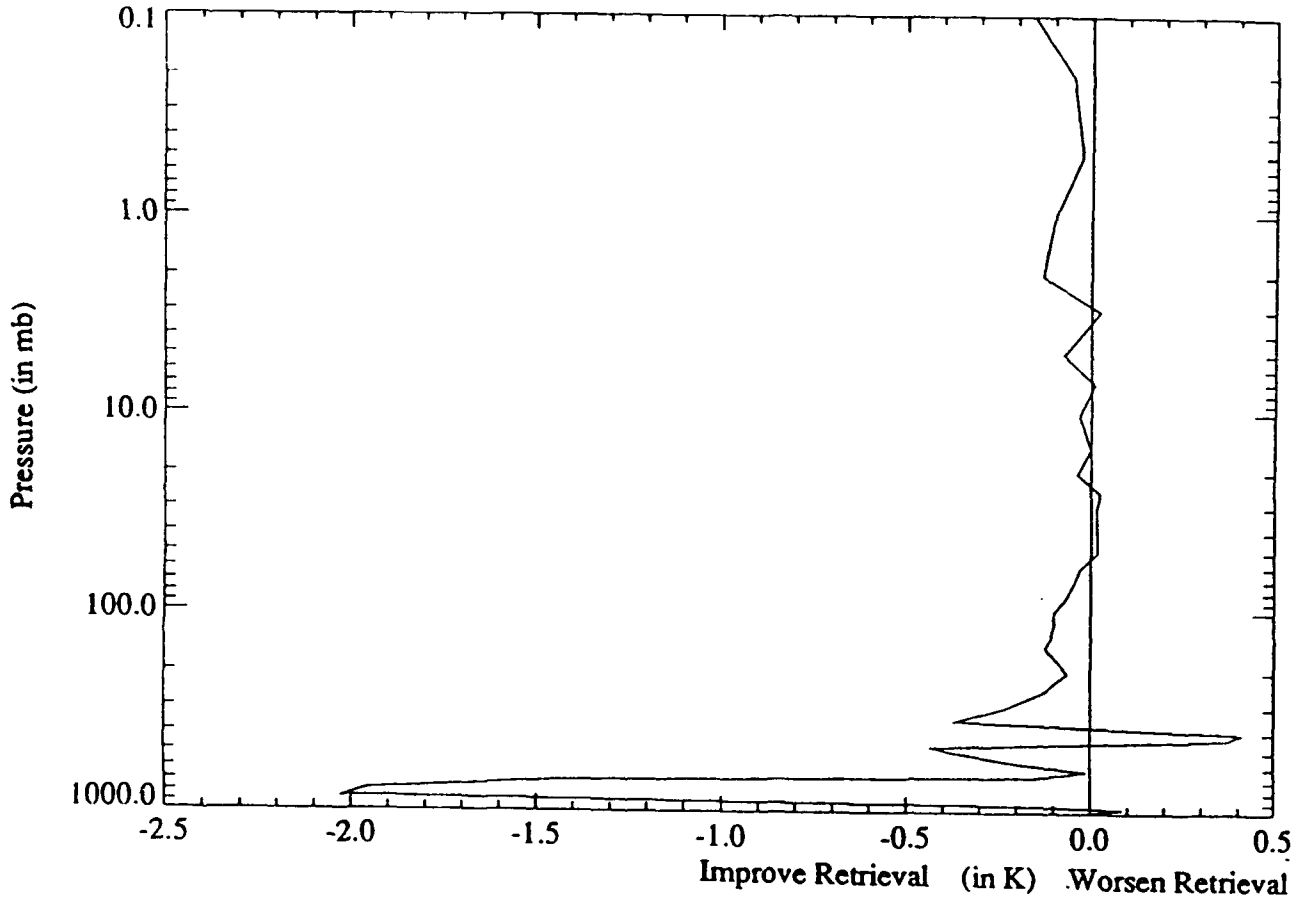

Figure 6: As for Fig. 3 except for a cloud top at 780 mb.

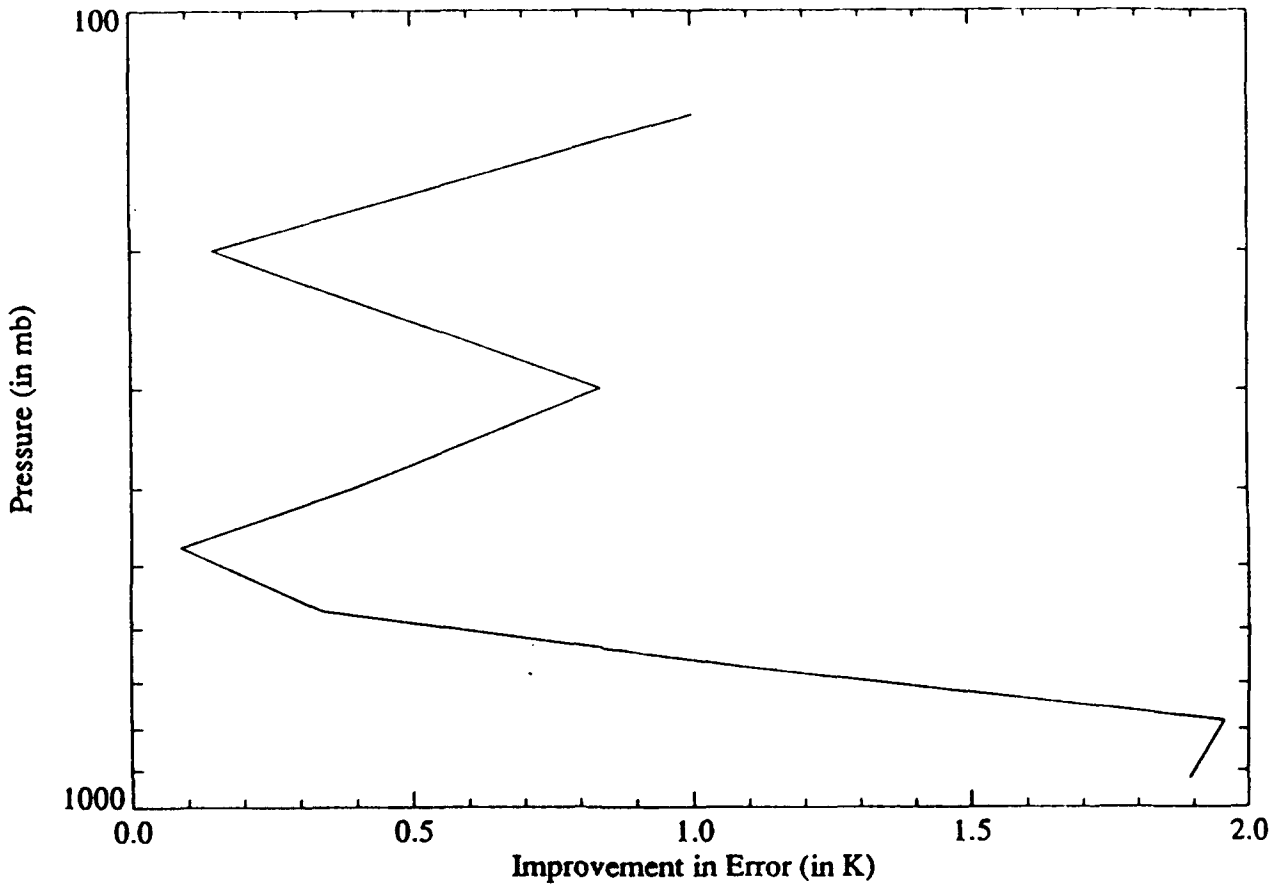

Figure 7: The improvement in the temperature retrieval at cloud top level as the cloud top altitude is varied. Cloud tops at approximately 100, 300 and 800 mb result in the largest improvement in the retrieval, because the peaks of the weighting functions are there.

improvement varies with the cloud top altitude and with the amount of small-scale variability in the temperature structure.

5.2 Role of Spaceborne Lidar in Satellite Cloud Retrievals

A significant component of global change is the predicted greenhouse warming caused by increasing atmospheric trace gases, including CO_2, N_2O, CH_4 and CFCs (IPCC report, 1990). Major uncertainties exist still, however, what the actual magnitude of this warming would be (e.g., Mitchell et al., 1989; Lindzen, 1990; Molnar and Wang, 1992), due to our inadequate nature of knowledge related to certain climate feedback processes. Admittedly, possibly the greatest uncertainty is associated with the behavior of clouds in response to climate perturbations (e.g., Cess et al., 1989; Arking, 1991). Clouds exert strong radiative effects, so their behavior can significantly affect atmospheric and oceanic processes on various spatial and temporal scales. For example, Webster and Stephens (1984) concluded that of all climate parameters, clouds have the largest possible effect on the radiation field, influencing Earth radiation budget, the heating of the ocean and the diabatic heating of the atmosphere. Hence, a global survey of cloud properties is a key objective of climate research programs.

Cirrus is a typical example of cloud types not well understood in relation to cloud-climate feedbacks (e.g., Liou, 1986; Stephens et al., 1990). Cirrus type clouds cover a climatically significant portion (at least 20%) of the globe. They are a prevailing cloud type over tropical oceans, and more and more new results indicate that thin cirrus covers a significantly larger fraction of the globe than previously thought (e.g., Prabhakara et al., 1988; Wylie and Menzel, 1989; Menzel et al., 1991). Since cirrus radiative forcing is significant, possible changes in its properties due to global change may have a profound effect on the predicted warming itself. Indeed, a General Circulation Model (GCM) simulation by Mitchell et al. (1989) pointed out that CO_2-doubling induced warming can induce phase changes in cirrus water content, leading to a significant negative feedback. More recently, Ramanathan and Collins (1991) have introduced the concept of a "cirrus limiting factor" which implies that the greenhouse warming will be limited by formation of highly reflective cirrus clouds over tropical oceans, shielding large amounts of solar radiation, limiting sea-surface temperature (SST) to temperatures no greater than around 305K.

Satellites can provide the necessary overview of cloud systems from the scales of synoptic weather systems to the scales of climate. The International Satellite Cloud Climatology Project (ISCCP) is to date the biggest effort to replace ground-based, "subjective"

cloud climatologies with a satellite-based, "objective" cloud data base (e.g., Rossow and Schiffer, 1991). However, retrieval of cirrus, especially *thin* cirrus, is notoriously difficult from satellite imagery using the current ISCCP techniques. Although as a part of ISCCP's intensive field observations (IFO) programs, extensive campaigns of coordinated measurements from satellites, aircraft and ground-based platforms were made of cirrus clouds, these campaigns have had limited spatial and temporal resolution. Additional series of measurements seems to be necessary to establish parameterizations of e.g., fractional cover, ice water content and vertical distribution of thin cirrus on large scales, important for global change studies. An objectively derived climatology of thin cirrus would provide a significant step toward achieving this goal.

There are existing methods to detect thin cirrus from satellite data. For example, Prabhakara et al. (1988) demonstrated the usefulness of the 10.8 mm and 12.6 mm channels of the infrared interferometer spectrometer (IRIS) aboard the Nimbus-4 satellite. Based on the large extinction differences between these two IRIS channels, they deduced mean seasonal maps of the distribution of thin cirrus over the oceans for the 50°N-50°S latitude belt. Infrared sounder data used primarily for retrieving atmospheric temperature profiles can also be used for identifying thin cirrus clouds (e.g. Smith and Woolf, 1976; McCleese and Wilson, 1976; Chahine et al., 1977; Molnar, 1981; Yeh, 1984). In fact, initial cirrus cloud climatologies have been created using this, so-called CO_2 Slicing Technique (Wylie and Menzel, 1989; 1991). Note, however, that the cirrus emissivity produced by these techniques is actually the product of 'real emissivity' (ϵ) and fractional cover (A_c) in the instrument's field-of-view (FOV).

Most recently, d'Entremont et al. (1992) illustrated the combined use of radiances measured by the Advanced Very High Resolution Radiometer (AVHRR) and by the High-Resolution Infrared Radiation Sounder (HIRS). Data from the AVHRR infrared (IR) window channels (Chs 3, 4 and 5) and coincident HIRS Chs 4-8 information (i.e. Chs used for the CO_2 Slicing Technique) were combined for retrieving *both* the emissivity and fractional cover of thin cirrus in a case study involving a Wisconsin cirrus IFO scene of the ISCCP program.

In summary, for the moment, we do not have a climatology of thin cirrus which makes distinction of actual fractional cover and emissivity. Nevertheless, ground-based (see Sassen, 1991 for a review) as well as airborne (Spinhirne et al., 1983) LIDAR measurements indicate that a spaceborne LIDAR could provide the most unambiguous detection of thin cirrus on a global scale. This is the consequence of significant improvement in laser technology, which has led to the development of LIDAR systems that use the scattered signal of a laser beam from

the atmosphere to identify atmospheric properties by various scattering and absorption processes. As far as clouds are concerned, they have proven to be especially useful for identifying cirrus, including thin and even subvisible cirrus (cf. Platt et al., 1987; Sassen, 1991). Unlike a satellite radiance pixel measured at a given wavelength, a LIDAR 'pixel' would clearly identify whether thin cirrus is present in the LIDAR-sounded atmospheric column, and its altitude and vertical extent (i.e. base height which cannot be inferred from IR radiances) would also be known. In addition, in the case of thin cirrus, the cloud top altitude of an underlying cloud layer (if any) could also be determined, contributing to the feasibility of satellite retrievals of certain 2-layered clouds systems. None the less, in this paper we will focus only on simpler cases, i.e. we will allow for a single cirrus layer (with variable fractional cover *and* emissivity) over an oceanic surface.

Here we discuss the potential usefulness of a spaceborne LIDAR system for creating a thin cirrus climatology when used in conjunction with a relatively novel satellite-based cloud retrieval scheme (called the Triangle Technique or TT for short) of the spatial-coherence type (Coakley and Bretherton, 1982).

In the next section, following a brief description of the TT (Molnar, 1983; 1992), we illustrate the problems this technique may face when applied to satellite imagery containing thin cirrus. In Section 5.2.2a, we present our main results, obtained from a series of Monte-Carlo simulations, to assess the potential gain obtainable due to the usage of the LIDAR-derived information to improve the TT-retrievals of thin cirrus over oceans. In Section 5.2.2b we mention potential uses of spaceborne LIDAR to improve objective oceanic cloud climatologies for such 2-layered cloud systems where one of the cloud layers is thin cirrus. We briefly discuss the results and indicate the directions of future work in the last section (5.2.3).

5.2.1 The TT retrieval method

The question arises why do we suggest a novel technique for *satellite imagery based* cloud retrievals in conjunction with the spaceborne LIDAR. The main reason is that conventional, i.e. fixed threshold techniques may have biases in the retrieved fractional cover because:

1. The fractional cloud cover is sensitive to the choice of threshold. Stowe and Pellegrino (1987), for example, have found inconsistencies between satellite cloud cover climatologies that they attribute primarily to differing choices for thresholds. This is especially

a problem when we want to create the longest possible satellite cloud climatology necessary for global change assessments.

2. The cloud cover is sensitive to data-resolution since errors in fractional cloudiness derived by using a fixed threshold depend not only on the cloud cover but also on cloud size (e.g., Coakley, 1987).

Clearly, a method which circumvents these problems would improve satellite cloud retrievals.

The Spatial Coherence Method (SCM) developed by Coakley and Bretherton (1982) seems to be a good candidate for more accurate cloud retrievals over oceans (homogeneity of surface required) because it is insensitive to data resolution when determining fractional cloud cover (Wielicki and Minnis, 1986; Wielicki et al., 1987). This is possible, since the SCM allows for clouds that only partially fill the sensor's FOV. Cloud layers can be detected and their characteristic emission and fractional cover can be determined by examining the spatial structure in plots of local standard deviation versus local mean radiance (Coakley and Bretherton, 1982). The so-called 'arch-feet' can be associated with cloudy and/or clear-sky radiances. In its original form, the SCM could retrieve fractional cloud cover only for single layered, *optically thick* oceanic cloud systems. Subsequent extensions allowed it to determine *daytime* fractional cloud cover for two-layered cloud systems, using visible spectral channel information in addition to the infrared channel (Coakley, 1983). Based on these works, Coakley and Baldwin (1984) have developed an objective analysis scheme for determining cloud cover over oceans, based solely on the application of the SCM. Nevertheless, for complex cloud systems the radiances associated with the cloud layers and/or the clear sky could not be reliably determined, so that they had to assign a "default estimate" to complex cloudiness, often with an unacceptably large error. Molnar and Coakley (1985) extended the SCM further to include multi-layered, *opaque* cloud systems based on *single*-channel information, thus allowing for *nighttime* retrievals.

Despite all these developments, the SCM still may fail in certain situations. For instance, marine stratus decks are often *sub-resolution everywhere* in a given scene, so no arch feet can form. This also can happen when the clouds are *not opaque* at the wavelength of the observation. This means that there is no arch foot for thin cirrus (transmissivity < 1) with variable emissivity in a given scene.

Addressing this problem, Molnar (1983) pointed out that the intersections of the upper envelope of an SCM-generated arch with the local mean standard deviation axis are associated with the radiances of the (uppermost) cloud layer and the surface. Consequently, even for complex cloud systems radiances associated with the clear sky and the uppermost cloud layer can be retrieved. Accordingly, for certain complex cloud formations, like marine stratiform cloud systems, which are often broken and thus appear to be subresolution for the satellite FOV, the fractional cloud cover can be derived from the radiance field. Like the SCM, this 'Triangle Technique' is also independent of sensor resolution and threshold. Moreover, it allows for retrievals even when the scene is so inhomogeneous that no arch feet are formed. Of course, in order to get reasonably accurate retrievals, the TT, like the SCM, also has to assume that the clouds to be retrieved reside in well-defined layers. Fortunately, this is exactly the case for both, climatically important, "difficult" cloud types: the top of marine stratiform clouds is essentially determined by the top of the marine boundary layer, whilst thin cirrus associated with deep convection has its top at the tropopause. In addition, because the TT does not require arch feet to form, it can analyze much smaller scenes than the SCM, so that the cloud top temperature and SST can be regarded constant within a given scene for these complex cloud systems. Thus, in principle, application of the TT could lead to a more accurate climatology of these cloud types than that obtained by methods based on threshold techniques or the SCM. Another issue that being based only *single* channel, IR window imagery data, the TT is equally applicable during daytime and nighttime.

Figure 8 illustrates the basic concept of the TT; when creating plots of local standard deviations versus local mean radiances, use *2 X 1* pixel-arrays (instead of the 2 X 2 or even larger arrays used in the SCM), in which case the upper-envelope of the "arch" is exactly a symmetrical triangle, 'sitting' on the local mean radiance axis. Intersections of this upper envelope with the local mean radiance axis are associated with the radiances of the (uppermost) cloud layer and the surface (or with an underlying *contiguous* cloud layer in case of a multilayered cloud system).

The case depicted on Fig. 8 shows a simulated TT-retrieval over a 'scene' of 1024 pixels with clear-sky radiance of 100 $mWm^{-2}SR^{-1}cm$ and cloud top radiance of 40 $mWm^{-2}SR^{-1}cm$. *Both* the cloud fraction and e are allowed to vary (in the [0.0,1.0] range) in this case. Note that, unlike the SCM, the TT is still able to determine the real cloud top radiance with a reasonable accuracy. However, it can only retrieve the effective cloud cover, which contributes to large errors if e is much smaller than 1. Furthermore, as Figs. 9 and 10 illustrate, for scenes where the cirrus is so thin that its emissivity varies in a range with upper

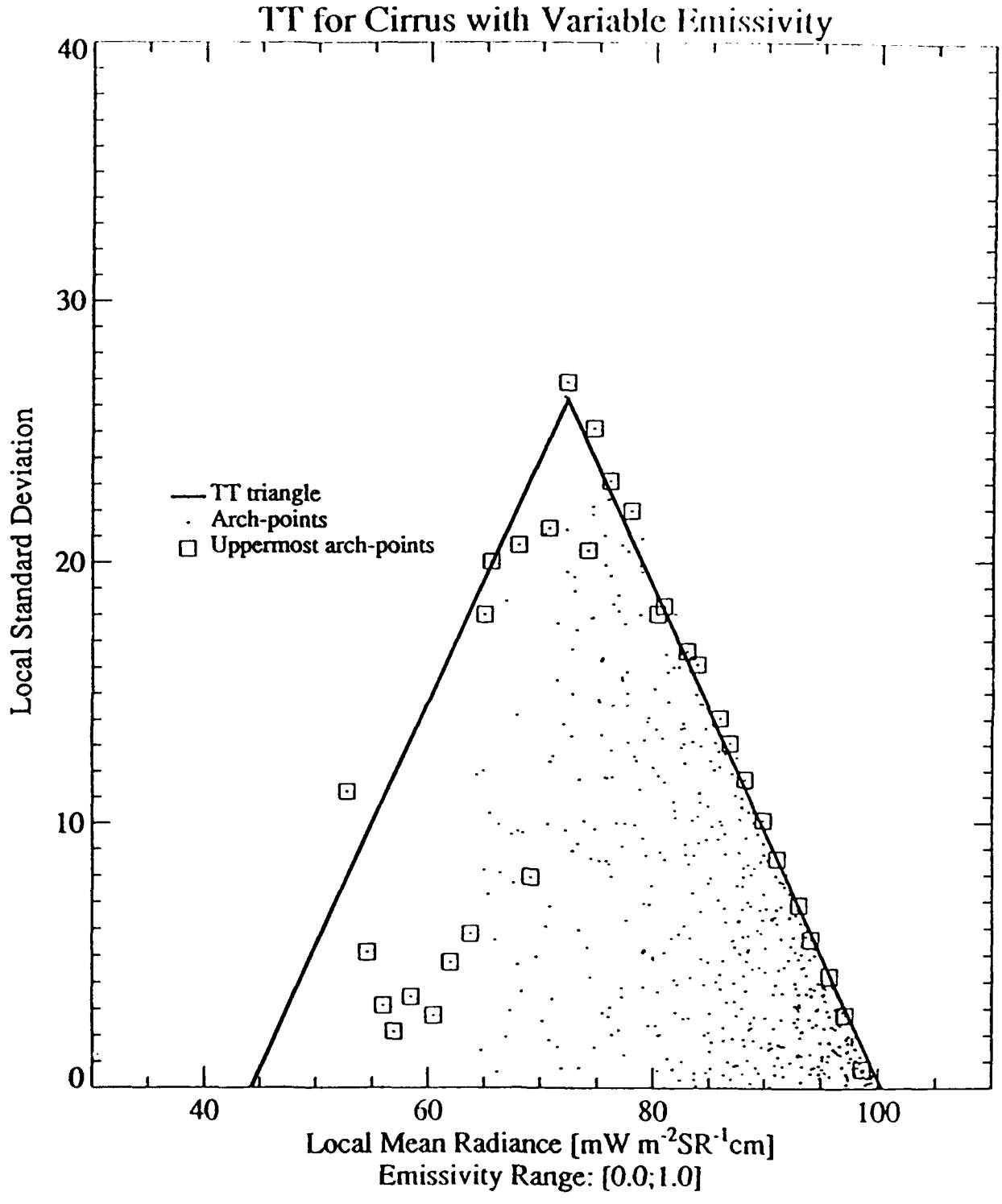

Figure 8: Illustration of TT-retrieval for cirrus with variable emissivity (range [0.0,1.0]) and cloud fraction (range [0.0,1.0]), with cloud top at 40 $mWm^{-2}SR^{-1}cm$. The clear-sky radiance associated with the surface is at 100 $mWm^{-2}SR^{-1}cm$.

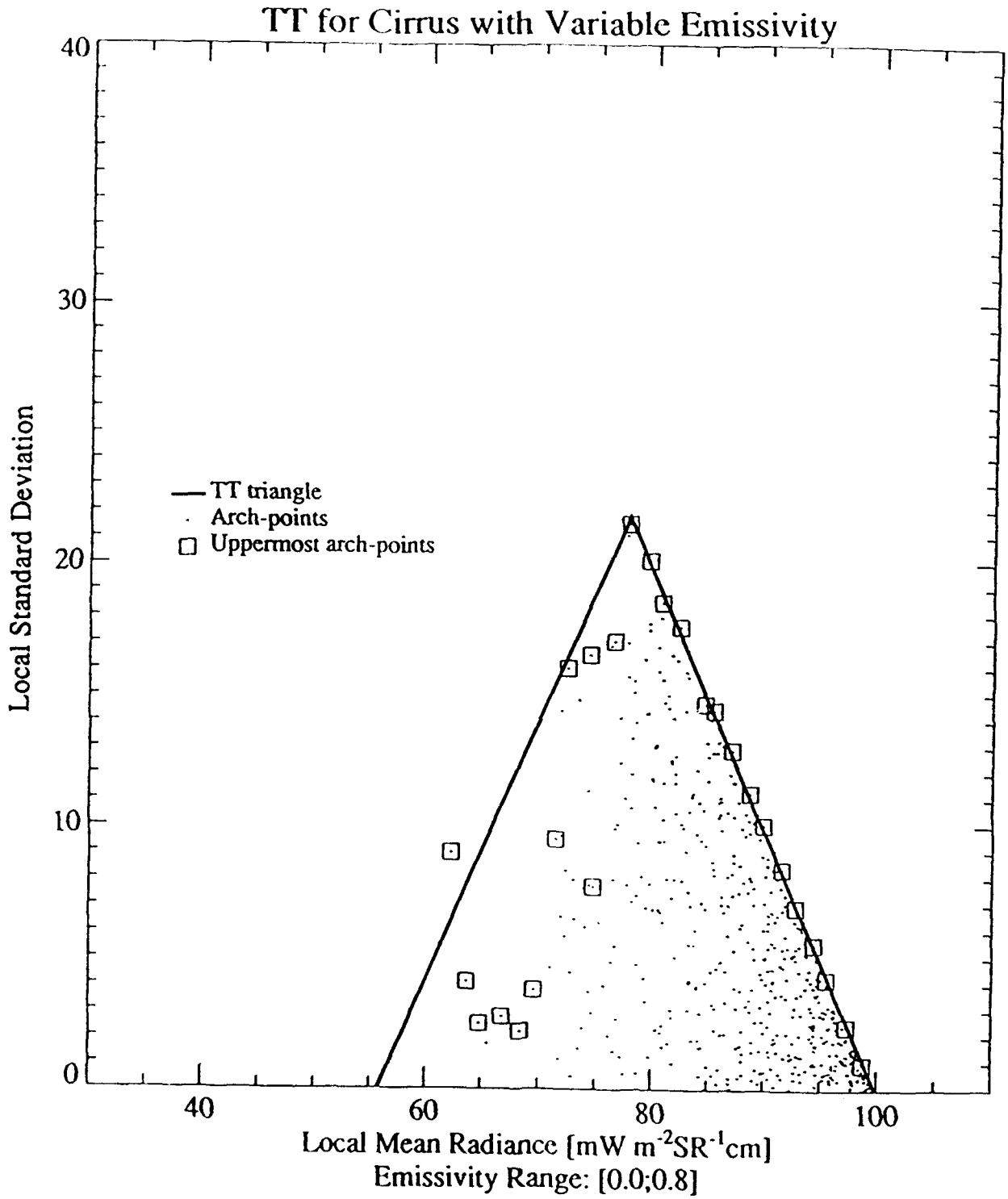

Figure 9: Same as Fig. 8 but the range of cirrus emissivity is [0.0,0.8].

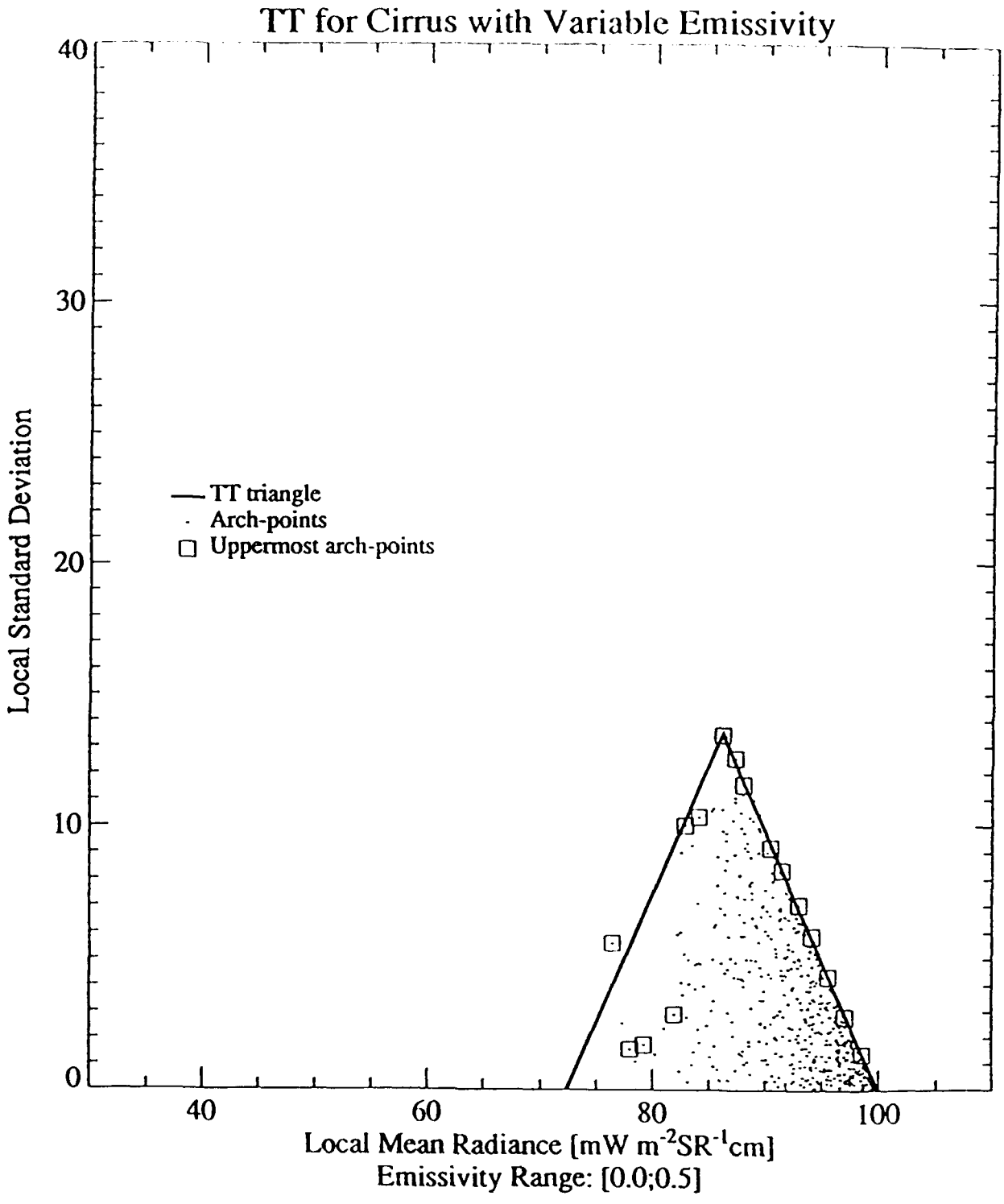

Figure 10: Same as Fig. 8 but the range of cirrus emissivity is [0.0,0.5].

limit significantly below 1, even the TT-retrieved cloud top radiance will have large errors. This is a clear indication that spaceborne LIDAR measurements could be extremely useful to improve the retrieval of cloud systems containing thin cirrus.

5.2.2 Results

a) Thin Cirrus over Oceans

We have performed a series of Monte-Carlo simulations to have first order quantitative estimates to what extent a spaceborne LIDAR system can improve the TT retrievals of thin cirrus.

In the most general case, both A_c and ϵ may vary from pixel to pixel. Consequently, the radiance (I_{av}) measured in the IR window (around 11 μm) for a given scene can be written as:

$$I_{av} = \epsilon A_c I_c + (1-\epsilon)A_c I_s + (1-A_c)I_s. \qquad (1)$$

Here, I_c is the radiance associated with the cloud top (spectral blackbody radiation at cloud top temperature), whilst I_s corresponds to the clear-sky radiation (i.e., surface spectral blackbody radiation, neglecting atmospheric attenuation for the moment at the IR window for the sake of simplicity). The ϵA_c quantity is referred to as the "effective emissivity" in the CO_2 Slicing Technique, whilst it is considered as "effective cloud cover" in satellite imagery. In the limiting case of A_c=1, the cirrus emissivity can be determined. Likewise, for ϵ=1 (opaque cloud), we have the cloud-fraction equation of the SCM.

For the "TT-only" case I_c and I_s are obtained from the TT, and the cloud cover is calculated as:

$$A_c = (I_{av}-I_s)/(I_c-I_s).$$

Note that this is actually an effective cloud cover in the simulated cases, but the TT does not "know" this when an I_c value corresponding to middle- (Fig. 9) or low-cloud (Fig. 10) is retrieved.

For the so-called "LIDAR+TT" case, I_c is the simulated spectral black-body radiance at cloud top (temperature at cloud top altitude is assumed to be known from aerological data), I_s is given by TT, and e is also considered known through the equation:

$$e = (I_s - I_{av})/(I_c - I_s) \qquad (2)$$

More precisely, e is the *average* emissivity determined from Eq. (2) for each of *those* IR radiance pixels where LIDAR FOVs indicate the *presence* of cirrus. Note that for such LIDAR FOVs A_c=1 is assumed. Consequently, in this case, for the whole scene, Eq. (1) gives:

$$A_c = (I_{av} - I_s)/(I_c - I_s)/e.$$

Note that for a simulated scene, the only "error" in the "LIDAR+TT" cloud fraction is caused by the error in the TT-retrieval of I_s. This is, of course, expected to be larger for scenes with larger cloud fractions and cirrus emissivities.

In the Monte-Carlo simulations to be described, we used an I_c=50 $mWm^{-2}SR^{-1}cm$ value, and I_s=100 $mWm^{-2}SR^{-1}cm$. The range of Ac variability is 0.4, centered at 0.2, 0.4, 0.5, 0.6 and 0.8 average cloud fractions, respectively. The range of emissivity variability is the widest possible, providing mean scene emissivities from 0.1 to 0.9 in 0.1 increments.

The results are summarized in Figs. 11 through 13. Figure 11 shows the errors of the cloud top radiance for the "TT-alone" case in %, relative to the "LIDAR+TT"-derived I_c (which, of course, has no error due to the accurate cloud-top altitude provided by the LIDAR). As expected, the error is largest, i.e. the improvement due to LIDAR use is the biggest for the smallest cloud fractions and emissivities. It is interesting to note that for low fractional cover, the LIDAR significantly improves the I_c-retrieval even for large e values. These results are only indicative in the sense that the relative error depends on the actual I_c value.

The simulations of cloud cover errors (in % of actual cover), however, were found to be independent of I_c, and so the relative A_c errors plotted in Figs. 12 and 13 are representing a general result, at least for the cloud fraction and emissivity *ranges* considered here. Comparing these figures indicates that very significant improvement can be attributed to LIDAR use for creating a fractional cloud cover climatology of thin cirrus. Figure 14 illustrates this point more clearly, depicting the *improvement* of A_c-retrievals due to LIDAR soundings.

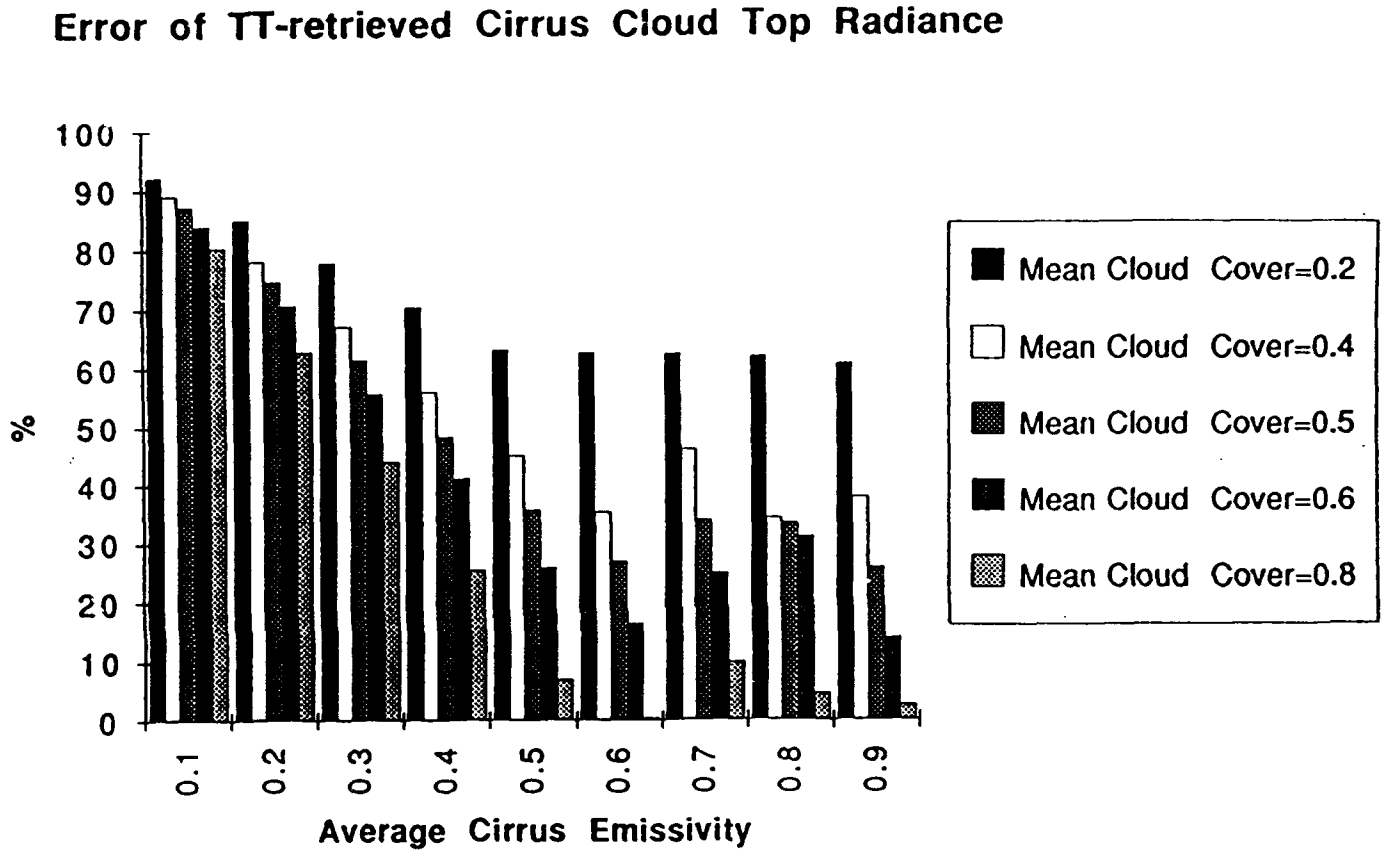

Figure 11: Error in TT-retrieved cirrus cloud top radiance as a function of mean scene cirrus emissivity and mean cloud fraction.

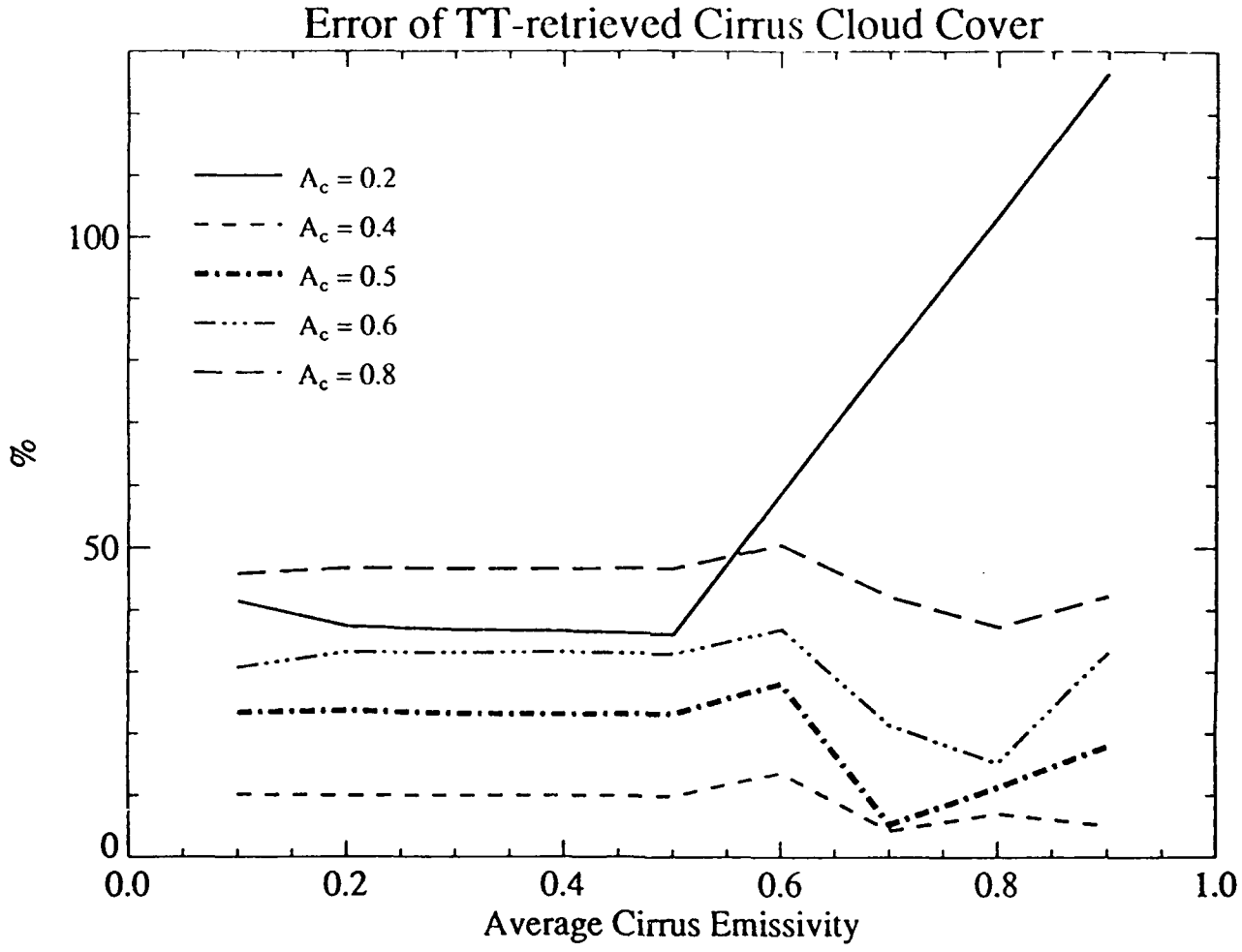

***Figure 12:** Error in TT-retrieved cirrus fractional cloud cover as a function of mean scene cirrus emissivity and mean cloud fraction.*

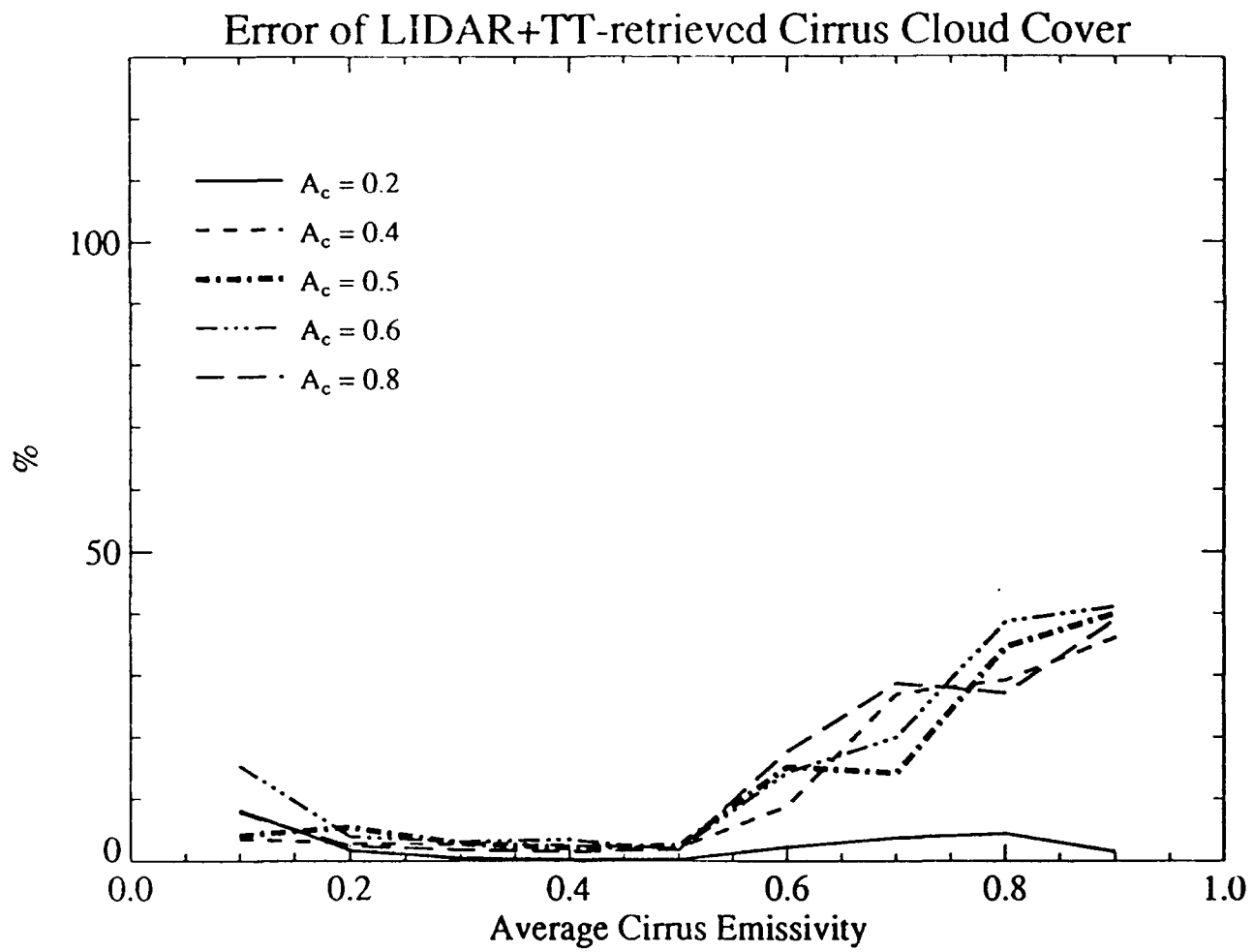

Figure 13: Error in LIDAR+TT-retrieved cirrus fractional cloud cover as a function of mean scene cirrus emissivity and mean cloud fraction.

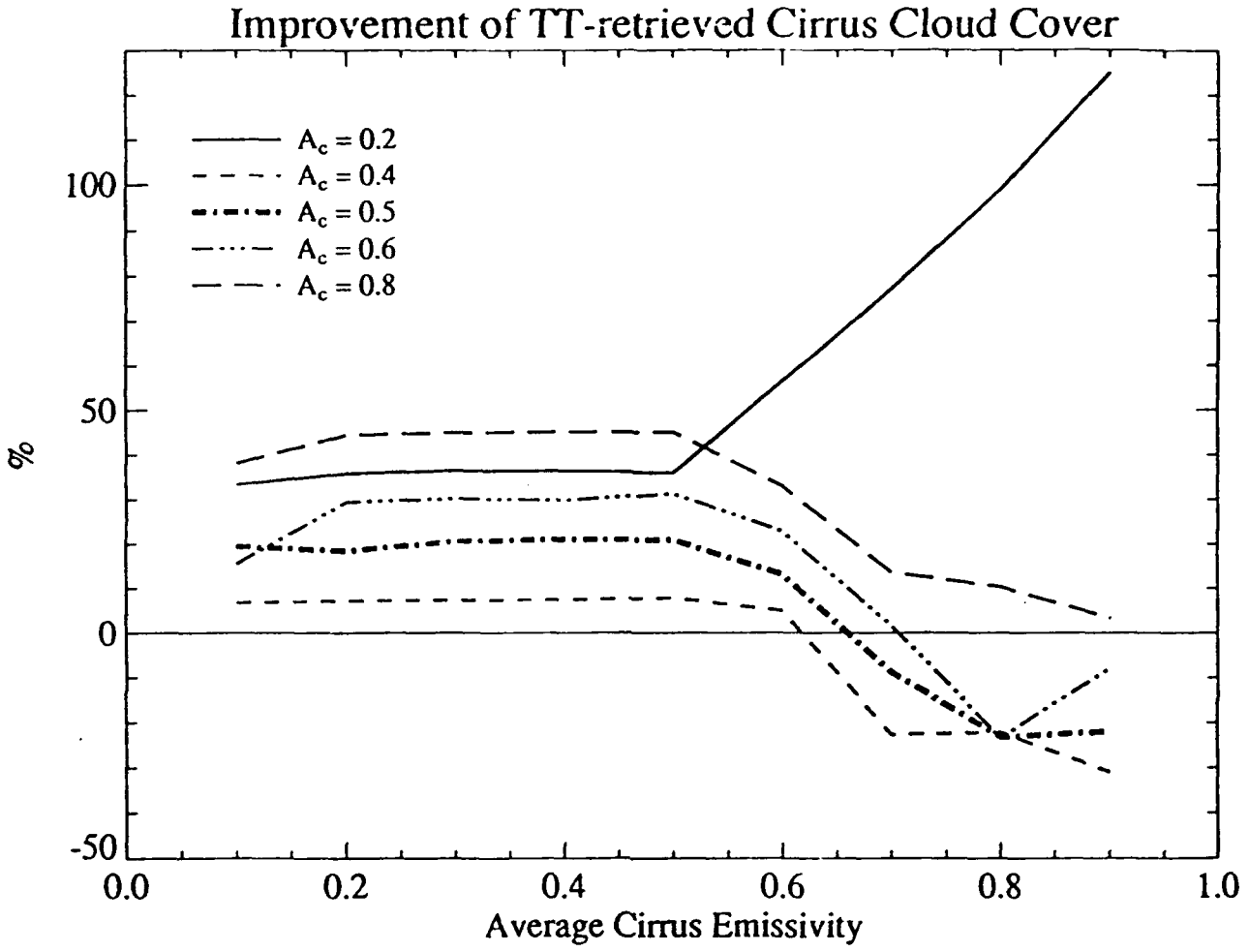

***Figure 14:** Improvement of error in TT-retrieved cirrus fractional cloud cover due to LIDAR use as a function of mean scene cirrus emissivity and mean cloud fraction.*

Note that for $\epsilon > 0.6$-0.7 and for cloud amounts around 0.5, the retrieval of A_c seems to be actually less accurate than for the "TT-alone" case. This is the result of 'compensating' errors in I_c and I_s retrievals using the TT alone. Moreover, for these cases, it is the cloud radiance which is "more erroneous", so, for example, the retrieved cloud would not even be regarded as thin cirrus, which would lead to a "distorted" cloud climatology.

b) Thin cirrus and Underlying Cloud Deck over Oceans

For thin cirrus, it is possible to obtain LIDAR backscatter associated not only with cirrus top and bottom but also with the top of an underlying cloud layer (if any). This would help to identify the radiance associated with the underlying cloud layer. The significance of this is clearly visible on Fig. 15, which shows the TT-retrieval of a scene where thin cirrus (with average emissivity of 0.5, 100% fractional cover and I_c=40 $mWm^{-2}SR^{-1}cm$) lies over a low-level, opaque cloud deck with 0.5 average cloud cover and a 90 $mWm^{-2}SR^{-1}cm$ cloud top radiance. Although the TT correctly indicates the radiances associated with the cirrus and the clear sky (at 100 $mWm^{-2}SR^{-1}cm$), there seems to be no indication whatsoever that a low-level deck is present. Thus, a coincident spaceborne LIDAR measurement would significantly increase our knowledge regarding cloud systems of this type.

5.2.3 Discussion and future work

Our preliminary results indicate that there is a definite usefulness and even a need for spaceborne LIDAR systems to improve our understanding of cloud/climate feedbacks, considered crucial for assessment of global change. This is especially true considering that the improvements illustrated through our Monte-Carlo simulations could be regarded as *lower* limits, since conventional cloud retrieval techniques (on which current satellite cloud climatologies are based) generally exhibit even larger errors than the TT. We plan, as a next step, to perform Monte-Carlo simulations for 2-layered systems mentioned in Section 3/b and analyze the results to assess the potential role of spaceborne LIDAR in this case.

6. CONCLUSIONS

This basic research program has: (a) investigated advanced observational philosophies for obtaining required meteorological parameters from spaceborne lidars, (b) assessed the potential impact of satellite lidar observations on numerical weather analysis and prediction models, and (c) studied the fusion of potential lidar sensor data with passive

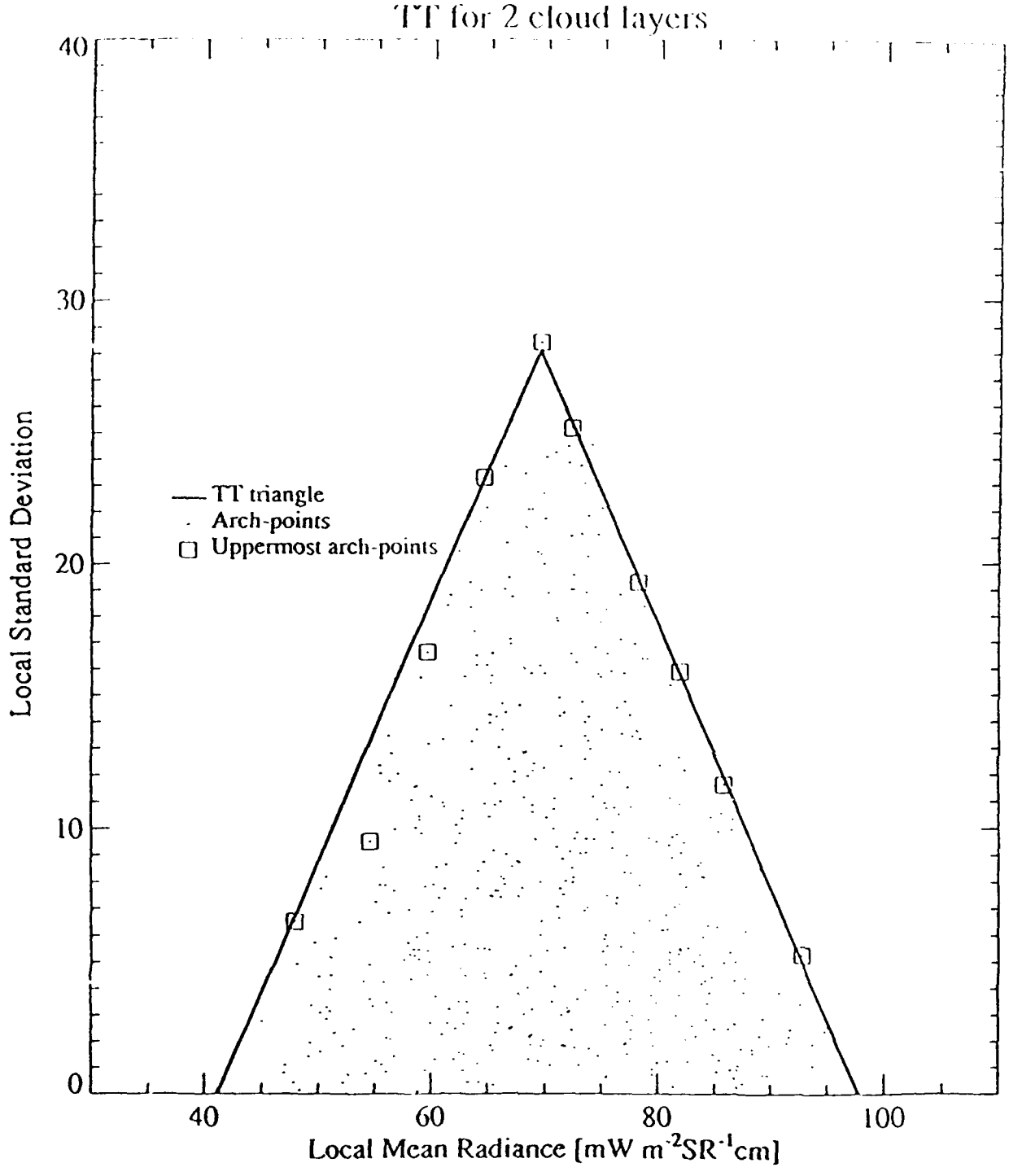

Figure 15. Illustration of TT-retrieval for a two-layer cloud system with cirrus and low-cloud layers. High cloud top corresponds to 40 $mWm^{-2}SR^{-1}cm$ whilst low cloud top is at 90 $mWm^{-2}SR^{-1}cm$. The clear-sky radiance associated with the surface is 100 $mWm^{-2}SR^{-1}cm$.

data from the existing Defense Meteorological Satellite Program (DMSP) suite of sensors with special emphasis on the retrieval and analysis of atmospheric winds, moisture, temperature, and clouds in support of tactical and strategic operations.

As the result of a trade-off of potential lidar systems for measuring meteorological parameters such as temperature, moisture, and winds, it was determined that maximum payback for NWP could be achieved by improving the accuracy and coverage of wind observations. To achieve this goal, two radically different instrument concepts were identified: (a) a combined stereo imager and cloud top lidar based on stereoscopic principles, and (b) a low power Doppler lidar. The stereo lidar will essentially provide super accurate height assignments of CDWs (since image correlation techniques will also be used). Since they will be available from a polar orbiter, coverage will be increased, especially for extratropical areas. The Doppler lidar will produce winds wherever there is a cloud and will likely provide boundary layer winds from maritime aerosol backscatter.

An OSSE was performed assuming an observational system capable of high accuracy winds at cloud top, through cirrus cloud layers, and in the marine boundary layer. Results of this experiment are summarized in Section 4.5 and in Grassotti et al. (1992). Based on examination of synoptic maps, time evolution of forecast and analysis error, and forecast error averaged over a number of individual 96 hour forecasts there were reductions in analysis and forecast errors for geopotential height, vector winds, zonal winds and humidity. These positive impacts were especially apparent in the Southern hemisphere where, for example, analysis and forecast errors of 500 hPa geopotential height were reduced by factors of 2-3, humidity forecasts with improved specification of the horizontal motion field resulted in better moisture forecasts, and there was a thirty percent reduction in the error of the 850 hPa zonal wind component with a forecast predictability improvement of up to 48 hours.

While our focus has been the impact of lidar based winds on the analysis and forecasting in the context of NWP, lidar information can also be used to improve the retrieval of other EDRs by exploiting active/passive sensor data fusion approaches. We have explored in some detail approaches to improve the retrieval of two important EDRs which are today obtained using passive data alone. These were: (a) using lidar cloud top height information to supplement a physical retrieval of temperature from SSM/T data; and (b) the use of the lidar to identify the presence of cirrus cloud to enhance the results of passive cloud property retrieval using a state-of-the-art spatial coherence technique. To

summarize the results which we have obtained: both experiments indicated that the lidar data could be used to improve the passive only retrieval of temperature or cloud, respectively:

- It was demonstrated that the ability to fix the temperature at cloud top could be used to constrain the physical inversion of temperature from an instrument such as the SSM/T. Operationally, it would be necessary to identify the presence of cloud from a combination of the lidar data and corresponding imagery. The enhancement would only be possible when cloud was present within the field-of-view.

- We have also illustrated that the availability of lidar data to identify cirrus cloud results in a significant improvement in cloud cover determination for low emissivity (e.g. subvisible) cirrus. A problem with current passive cloud analysis approaches is the difficulty in delineating non-unit emissivity cirrus cloud. The results of Section 5.2 illustrate the feasibility of using both passive imager and lidar data to delineate areas where non-unit emissivity cirrus are present which are extremely difficult to sense using passive data alone. Notably, the data fusion advantages cited above come at no additional hardware cost above that required to obtain the wind data.

While the overall results of this study are preliminary, we conclude that simple satellite borne lidar applications such as that described here can enhance the capability of the overall DMSP system to fulfill its mission by providing better quality measurements to support numerical weather prediction and other meteorological applications.

7. REFERENCES

Arking, A., 1991: The Radiative Effects of Clouds and their Impact on Climate. *Bull. Am. Met. Soc.*, **71**, 795-813.

Arnold, C.P., and C.H. Dey, 1986: Observing systems simulation experiments: Past, present, and future. *Bull. Amer. Meteoro. Soc.*, *67*, 687-695.

Atlas, R., E. Kalnay, W.E. Baker, J. Susskind, D. Reuter, and M. Halem, 1985: Observing systems simulation experiments at GSFC. In W.E. Baker and R.J. Curran, editors, *Global Wind Measurements*, pages 65-71. A. Deepak Publishing, Hampton, VA.

Baker, W.E. and R.J. Curran, (eds), 1985: Global Wind Measurements, *ESA Journal 1987, 11*, A. Deepak Publishing, Hampton, VA.

Baker, W. E., 1992: Science Goals and Mission Objectives of NASA's Laser Atmospheric Wind Sounder Program. 16th International Laser Radar Conference. NASA Conference Publication 3158, pp. 251-255.

Brenner, S., C.-H. Yang and S.Y.K. Yee, 1982: The AFGL spectral model of the moist global atmosphere: Documentation of the baseline version. AFGL-TR-82-0393, AFGL, 65 pp. [NTIS ADA129283]

Brenner, C.-H. Yang and K. Mitchell, 1984: The AFGL global spectral model: Expanded resolution baseline version. AFGL-TR-84-0308, AFGL. [NTIS ADA160370]

Cess, R. D., et al., 1989: Interpretation of Cloud-Climate Feedback as Produced by 14 Atmospheric General Circulation Models. *Science*, **245**, 513-516.

Chahine, M. T., H. H. Aumann, and F. W. Taylor, 1977: Remote sensing of cloudy atmospheres. Part III: Experimental verification. *J. Atmos. Sci.*, **34**, 758-765.

Coakley, J. A., Jr., 1983: Properties of multilayered cloud systems from satellite imagery. *J. Geophys. Res.*, **88**, 10818-10828.

Coakley, J. A., Jr., 1987: A Dynamic Threshold Method for Obtaining Cloud Cover from Imagery Data, *J. Geophys. Res.*, **92**, 3985-3990.

Coakley, J. A., Jr., and F. P. Bretherton, 1982: Cloud cover from high-resolution scanner data: Detecting and allowing for partially filled fields of view. *J. Geophys. Res.*, **87**, 4917-4932.

Coakley, J. A., Jr., and D. G. Baldwin, 1984: Towards the objective analysis of clouds from satellite imagery data. *J. Clim. Appl. Meteorol.*, **23**, 1065-1099.

Curran, R. J., 1989: "NASA's plans to observe the Earth's atmosphere with lidar." *IEEE Trans. Geosci. Remote Sensing* **27**: 154-163.

Curran, R.J., et al., 1988: *LAWS Instrument Panel Report*, NASA, Wash. DC, 55 pp.

d'Entremont, R. P., D. P. Wylie, J. W. Snow, M. K. Griffin, and J. T. Bunting, 1992: Retrieval of Cirrus Radiative and Spatial Properties Using Independent Satellite Data Analysis Techniques. In *Preprints, Sixth Conference on Satellite Meteorology and Oceanography*, Jan. 5-10, Atlanta, GA, *AMS, Boston*, pp. 17-20.

Daley, R., 1980: "On the optimal specification of the initial state for deterministic forecasting." *Mon. Wea. Rev.* 108: 1719-1735.

Dey, C.H. and L.L. Morone, 1985: Evolution of the National Meteorological Center Global Data Assimilation System: January 1982 - December 1983. *Monthly Weather Review*, 113:304-318.

Geleyn, J.-F.,1981: Some diagnostics of the cloud radiation interaction in ECMWF forecasting models. In workshop on Radiation and Cloud-Radiation Interaction in Numerical Modeling, ECMWF, Reading, UK, pp. 135-161.

Grassotti, C., R. G. Isaacs, R. N. Hoffman, M. Mickelson, T. Nehrkorn, J.-F. Louis, 1991: A Simple Doppler Wind Lidar Sensor: Simulated Measurements and Impacts in a Global Assimilation and Forecast System. PL-TR-91-2253, Phillips Laboratory, Hanscom AFB, MA 01731, 98 pp.

Heymsfield, A.J.and C.M.R. Platt, 1984: A parameterization of the particle size spectrum of ice clouds in terms of the ambient temperature and the ice water content. *J. Atmos. Sci., 41,* 5, pp. 846-855.

Hoffman, R.N. et al., 1989: Satellite enhanced numerical weather prediction. *GL-TR-89-0099.* ADA210108

Hoffman, R.H., C. Grassotti, R.G. Isaacs, J.-F. Louis, T. Nehrkorn and D.C. Norquist, 1990: Assessment of the Impact of Simulated Satellite Lidar Wind and Retrieved 183 GHz Water Vapor Observations on a Global Data Assimilation System. *Monthly Weather Review, 118,* 12, 2513-2542.

Hogan, D. B., A. Rosenberg and B. H. Cohen, 1983: *Analysis of a space-based differential absorption lidar for simultaneous measurements of temperature and humidity profiles.*

Huffaker, R.M. et al., 1984: Feasibility studies for a global wind measuring satellite system (WINDSAT); analysis of simulated performance. *Appl. Optics, 23,* 2523.

Intergovernmental Panel on Climate Change (Houghton et al. eds.), 1990: Climate Change: The IPCC Scientific Assessment. *WMO, UNEP, Cambridge University Press,* Cambridge.

Lindzen, R.S., 1990: Some Coolness about Global Warming. *Bull. Am. Met. Soc.,* **71,** 288-299.

Liou, K.-N., 1986: Influence of Cirrus Clouds on Weather and Climate Processes: A Global Perspective. *Mon Wea. Rev.,* **114,** 1167-1199.

Liou, K.N., Y. Takano. S.C. Ou, A. Heymsfield, and W. Kreiss, 1990: Infrared transmission through cirrus clouds: a radiative model for target detection. Applied Optics, 29, 13, pp. 1886-1896.

McCleese, D. J., and L. S. Wilson, 1976: Cloud top heights from temperature sounding instruments. *Quart. J. Roy. Met. Soc.,* **102,** 781-790.

Menzel, W. P., D. P. Wylie, and K. I. Strabala, 1991: Seasonal and diurnal changes in cirrus clouds as seen in four years of observations with the VAS. Submitted to *J. Appl. Met.*

Menzies, R.T. and D.M. Tratt, 1991: Aerosol and cloud observations with a CO_2 backscatter lidar on the NASA DC-8 GLOBE Pacific missions. Preprint Volume of the Seventh Symposium on Meteorological Observations and Instrumentation, American Meteor. Society, Boston Mass.

Mitchell, J. F. B., Senior, C. A., and W. J. Ingram, 1989: CO_2 and Climate: A missing Feedback? *Nature,* **341,** 132-134.

Molnar, G., 1981: Estimation of cloud top height and effective cloud cover from infrared satellite soundings. *Adv. Space Res.*, **1**, 323-326.

Molnar, G., 1983: Application of the spatial coherence method for the treatment of subresolution and cirrus clouds. *Preprint Volume: Fifth Conference on Atmospheric Radiation*, Oct. 31-Nov. 4, 1983, Baltimore, MD. AMS Publication, pp. 276-279.

Molnar, G., 1992: Satellite Retrievals of Marine Stratiform Cloud Systems. In *Preprints, Sixth Conference on Satellite Meteorology and Oceanography*, Jan. 5-10, Atlanta, GA, *AMS, Boston*, pp. 7-10.

Molnar, G., and J. A. Coakley, Jr., 1985: Retrieval of cloud cover from satellite imagery data: A statistical approach. *J. Geophys. Res.*, **90**, 12960-12970.

Molnar, G., and Wang, 1992: Effects of Cloud Optical Property Feedbacks on the Greenhouse Warming. Accepted by *J. Climate.*

Platt, C.M.R., and A.C. Dilley, 1981: Remote sounding of high clouds. IV: Observed temperature variations in cirrus optical properties. *J. Atmos. Sci., 38*, 1069-1082.

Platt, C. M. R., J. C. Scott, and A. C. Dilley, 1987: Remote Sounding of High Clouds. Part VI: Optical Properties of Midlatitude and Tropical Cirrus. *J. Atmos. Sci.*, **44**, 729-747.

Prabhakara, C., R. S. Fraser, G Dalu, Man-Li C. Wu, R. J. Curran, and T. Styles, 1988: Thin Cirrus Clouds: Seasonal Distribution over Oceans Deduced from Nimbus-4 IRIS. *J. Appl. Met.*, **27**, 379-399.

Ramanathan, V., and W. Collins, 1991: Thermodynamic regulation of ocean warming by cirrus clouds deduced from observations of the 1987 El Nino. *Nature*, **352**, 27-32.

Rossow, W. B., and R. A. Schiffer, 1991: ISCCP Cloud Data Products. *Bull. Am. Meteorol. Soc.*, **72**, 2-20.

Salvetti, G., 1987: "Spaceborne doppler wind lidars." *ESA Journal* , **11-12**: 19-36.

Sassen, K., 1991: The Polarization Lidar Technique for Cloud Research: A Review and Current Assessment. *Bull. Am. Met. Soc.*, **72**, 288-299.

Smith, W. L., and H. M. Woolf, 1976: The use of eigenvectors of statistical covariance matrices for interpreting satellite sounding radiometer observations. *J. Atmos. Sci.*, **33**, 1127-1140.

Spinhirne, J. D., M. Z. Hansen and J. Simpson, 1983: The structure and phase of cloud tops as observed by polarization lidar. *J. Climate Appl. Meteor.*, **22**, 173-176.

Spinhirne, J.D., S. Chudamani, J.F. Cavanaugh, 1991: Visible and near IR lidar backscatter observations on the GLOBE Pacific survey missions. Preprint Volume

of the Seventh Symposium on Meteorological Observations and Instrumentation, American Meteor. Society, Boston Mass.

Stephens, G. L., S.-C. Tsay, P. W. Stackhouse, Jr., and P. J. Flatau, 1990: The Relevance of the Microphysical and Radiative Properties of Cirrus Clouds to Climate and Climate Feedback. *J. Atmos. Sci.*, **47**, 1742-1753.

Stowe, L. L., and P. P. Pellegrino, 1987: Intercomparison of Nimbus-7 and ISCCP Cloud Data Sets. In *"Clouds and Climate II,"*WMO/NASA/NSF/NOAA/DOE, 1987, 43.

Takano, Y., and K.-N. Liou, 1989: Solar radiative transfer in cirrus clouds. Part I: Single-scattering and optical properties of hexagonal ice crystals. *J. Atmos. Sci., 46*, 1, pp. 3-19.

Warren, S.G., 1984: Optical constants of ice from the ultraviolet to the microwave. *Appl. Optics*, 23:8, 1206-1225.

Webster, P. J., and G. L. Stephens, 1984: Cloud-radiation interaction and the climate problem. In *The Global Climate*, edited by J. Houghton, Cambridge University Press, New York, 63-78.

Weinman, J., 1985: Private Communication.

Wielicki, B. A., and P. Minnis, 1986: The effect of spatial resolution on satellite derived cloud cover. *Preprints for the Sixth Conference on Atmospheric Radiation*, Williamsburg, VA, May 13-16, AMS, pp. 85-59.

Wielicki, B. A., L. Parker, and C. Tolson, 1987: The Effect of Spatial Resolution on Satellite Derived Cloud Properties. In *"Clouds and Climate II"*, WMO/NASA/ NSF/NOAA/DOE, 1987, 75.

Woodbury, G.E. and M.P. McCormick, 1986: Zonal and geographical distributions of cirrus clouds determined from SAGE data. *J. Geophys. Res., 91* D2, pp. 2775-2785.

Wylie, D., and W. P.Menzel, 1989: Two years of cloud cover statistics using VAS. *J. Climatol.*, **2**, 380-392.

Wylie, D., and W. P.Menzel, 1991: A cirrus climatology from NOAA/HIRS. *Paleogeog., Paleocli., Paleoeco.*, **90**, 49-53.

Yeh, H. Y., 1984: Determination of cloud parameters from infrared sounder data. *J. Geophys. Res.*, **89**, 11759-11770.

8. ACKNOWLEDGEMENT

The authors thank their colleagues D. Hogan and D. Kenyon at GE Astro Space Division, Princeton, NJ for providing lidar wind error estimates. We also acknowledge the report processing and organizational talents of E. Stenhouse of AER.

9. APPENDIX - PUBLICATIONS AND PRESENTATIONS AS A RESULT OF THIS EFFORT

Isaacs, R. G., C. Grassotti, R.N. Hoffman, J.-F. Louis, and T. Nehrkorn, 1991: *Development of a Simple Lidar Wind Sounder Data Set for Use in Observing System Simulation Experiments*. Special Session on Laser Atmospheric Studies, 71st AMS Annual Meeting, American Meteorological Society, New Orleans, LA.

Isaacs, R. G., C. Grassotti, R. N. Hoffman, M. Mickelson, T. Nehrkorn, J.-F. Louis, 1991: *NWP impact of cloud top and boundary layer winds from a satellite borne lidar: an Observing System Simulation Experiment,* Paper presented at CIDOS-91, Cloud Impacts on DoD Operations and Systems 1991 Conference. Aerospace Corporation, El Segundo, CA, 9-12 July 1991.

Grassotti, C., R. G. Isaacs, R. N. Hoffman, M. Mickelson, T. Nehrkorn, J.-F. Louis, 1991: *A Simple Doppler Wind Lidar Sensor: Simulated Measurements and Impacts in a Global Assimilation and Forecast System.* PL-TR-91-2253, Phillips Laboratory, Hanscom AFB, MA 01731, 98 pp.

Isaacs, R. G., C. Grassotti, R. N. Hoffman, M. Mickelson, T. Nehrkorn, J.-F. Louis, 1991: *NWP impact of cloud top and boundary layer winds from a satellite borne lidar: an Observing System Simulation Experiment, Proceedings of the 16th International Laser* Radar Conference, Massachusetts Institute of Technology, NASA Conference Publication 3158, pp. 377-380.